



Controls over debris flow initiation in glacio-volcanic environments in the Southern Andes

Ivo Fustos-Toribio¹, Daniel Basualto³, Ardy Gatica¹, Alvaro Bravo-Alarcón^{2,1}, José-Luis Palma⁴, Gabriel Fuentealba^{5,2}, and Sergio A. Sepúlveda^{6,7}

¹Departamento de Ingeniería en Obras Civiles, Facultad de Ingeniería y Ciencias, Universidad de La Frontera, Francisco Salazar #01145, Temuco, Chile

²Programa de Magíster en Ciencias de La Ingeniería, Universidad de La Frontera, Temuco, Chile

³Departamento de Ingeniería Eléctrica, Facultad de Ingeniería y Ciencias, Universidad de La Frontera, Francisco Salazar #01145, Temuco, Chile

⁴Departamento Ciencias de la Tierra, Facultad de Ciencias Químicas, Universidad de Concepción, Víctor Lamas 1290, Concepción, Chile

⁵Ministerio del Interior, Temuco, Chile

⁶Departamento de Geología, Facultad de Ciencias Físicas y Matemáticas, Universidad de Chile, Santiago, Chile

⁷Department of Earth Sciences, Faculty of Science, Simon Fraser University, Burnaby, Canada

Correspondence: Daniel Basualto (daniel.basualto@ufrontera.cl)

Received: 24 March 2025 – Discussion started: 9 April 2025

Revised: 1 September 2025 – Accepted: 12 November 2025 – Published: 5 December 2025

Abstract. The Southern Andes is an active zone of mass wasting processes with unknown constraints for public policies. Several conditioning factors could have an impact on the generation of debris flows, being controlled by water accumulation. This study investigates the generation of the Ñisoleufu debris flow, an active area of debris flow generation in Southern Andes, reviewing the interplay between geomorphological, geotechnical and hydrometeorological controls in debris flow dynamics, focusing on the effects of soil properties, slope characteristics and precipitation events.

Our results highlight significant changes in soil moisture content on critical days associated with debris flow events. We revealed that the combination of areas with high water accumulation capacity from local runoff and slopes that capture precipitation effectively were crucial in the generation of debris flows. Areas with granular volcanic soils acted as storage mediums for water, which, coupled with decreased shear strength, facilitated debris flow initiation. The thin and fine-grained layers of glacial deposits located beneath the volcanic soil, characterized by low hydraulic conductivity, created localized accumulation zones that reinforced the storage capacity of adjacent areas, particularly in pyroclastic volcanic deposits in the release zone. The hydraulic properties

of the volcanic deposits suggest that water storage capacity and high hydraulic conductivity play a critical role in rainfall-induced debris flow initiation. Additionally, we observed that the debris flow of the Ñisoleufu event has evidence of reworked lapilli-sized particles (> 5 mm), being consistent with the surface and shallow water movement that reduces the slope stability within the area.

Analysis of ERA5-land dataset showed abrupt changes in soil moisture content at various depths and time periods, correlating with intense or prolonged rainfall events. These results underscore the role of geomorphological features in modulating soil moisture and thereby affecting the stability and movement of debris flows. Our results provide a comprehensive understanding of how geomorphology interacts with hydrological factors to influence debris flow behaviour in volcanic areas of the Southern Andes for the first time. Overall, the research highlights the critical role of geomorphological and hydrological factors in debris flow generation and dynamics. It emphasizes the need for incorporating detailed soil and slope characteristics into models for predicting debris flow risks. By understanding the combined effects of water accumulation, soil properties, and slope dynamics, this study contributes valuable insights into managing and

mitigating debris flow hazards in vulnerable regions. These findings enhance the predictive capacity for rainfall-induced debris flows and provide practical criteria for hazard assessment in post-glacial volcanic terrains.

1 Introduction

Episodes of extreme rainfall have increased due to climate change, resulting in a greater frequency of debris flows (Jakob and Lambert, 2009; Lee, 2017; Fustos et al., 2017; Dey and Sengupta, 2018) and mainly related to fast changes of soil water content (Fustos-Toribio et al., 2021). Currently, mass wasting processes produce widespread damages, representing a significant threat to human life (Sepúlveda and Petley, 2015; Vega and Hidalgo, 2016). Consequently, the need to forecast (Fustos et al., 2020a) and mitigate (Fustos-Toribio et al., 2021) the effects of these events has become a high priority for governments facing increasing episodes of rainfall-induced landslides linked with climate change. An accurate assessment of potential debris flows to regional scale needs precise understanding of their triggering and controlling conditions. Therefore, we assessed the main conditioning and triggering conditions of debris flows in Southern Andes in order to understand their evolution from stable slope to mass wasting event.

Worldwide, the increasing frequency and intensity of such extreme precipitation events exacerbated by climate change to regional scale (Stoffel et al., 2013; Pavlova et al., 2014) introduce severe threats to human life and property. Changing precipitation patterns related to extreme precipitation, lead to conditions conducive for debris flows in wide areas in North America (Bovis and Jakob, 1999), Asia (Chang et al., 2017), Europe (Malet et al., 2005; Stoffel et al., 2013; Pavlova et al., 2014) and South America (Sepúlveda, 2013; Sepúlveda et al., 2014; Fustos-Toribio et al., 2022). Stand out heavy tropical storms, such as Taiwan, increasing debris flow incidents (Chang et al., 2025) and compromising the safety of urban areas located near mountainous terrains (Chen et al., 2015; Kang et al., 2017). The Wenchuan Earthquake in China exemplifies how seismic activity can trigger extensive debris flows, resulting in not only immediate destruction but also long-lasting hazards due to the formation of landslide-dammed lakes that threaten downstream communities (Cui et al., 2009; Wang and Yu, 2015). Accurate forecasting of debris flow events is vital for disaster preparedness and mitigation. Understanding the triggering conditions – including rainfall intensity, groundwater levels, and geological features – is essential for developing conceptual models that represent the regional conditions that could control a debris flow initiation. Debris flows are influenced by soil hydraulic characteristics and the intensity/duration of rainfall events (Singh and Kumar, 2020), in which rainfall intensities serve as crucial predictors in mountainous regions (Chang et al., 2017;

Fustos-Toribio et al., 2022). Moreover, coarse-grained volcanic soils exhibit transient increases in pore pressure during intense rainfall events (Huang et al., 2012). Conversely, fine-grained soils with low infiltration rates do not experience significant changes in the pore pressure, generating failures due to decreased soil shear strength (Dahal and Hasegawa, 2008; Dahal et al., 2011). Hence, understanding soil composition and granulometric features is pivotal in assessing debris flow susceptibility worldwide. Debris flows are mainly controlled by the geomorphological features and the specific geological evolution of each region of the planet, highlighting the need for localized and context-specific approaches for their study and management. One of the next frontier corresponds to constrain the debris flow generation in glacial environments under changing precipitation events related to climate change.

Nowadays, understanding the impact of debris flows in glacial environments becomes critical in the Chilean southern Andes, particularly due to the most part of the inhabitants live there. Changes of precipitation patterns related to climate change, particularly fast and intense rainfall events, could amplify the frequency and magnitude of debris flows (Fustos-Toribio et al., 2022). An increase of extreme hydrometeorological events affecting slopes in glacial settings is observed, whose mechanical properties and geomorphology have evolved since the Last Glacial Maximum (Fustos-Toribio et al., 2021; Somos-Valenzuela et al., 2020; Ochoa-Cornejo et al., 2024). Considerable uncertainty remains about how the interaction between volcanic-derived soils over glacial landforms will respond to extreme hydrometeorological events. One of the current models for initiation of debris flows is related to slow deforming surfaces in hillslopes, mainly due to gravity and surface erosion during high precipitation events (Xie et al., 2020; Yi et al., 2021). Slow surface deformation could lead to extensional failures that could expand and deepen, generating landslides and evolving into debris flows, especially under water-saturated conditions or heavy rainfall (Gregoretti, 2000; Fustos et al., 2017; Wang et al., 2024). The capacity to oversee these extensional failures in remote areas close to roads is an open question yet, mainly in Southern Andes.

Historical debris flow events in the Southern Andes remain subject to uncertain conditioning factors. The transformation of landslides into debris flows typically occurs when sliding material incorporates water, significantly increasing its fluidity – as observed in the Villa Santa Lucía event in Chilean Patagonia (Somos-Valenzuela et al., 2020). The occurrence of debris flows in volcanic settings is of considerable scientific interest (Cheung and Giardino, 2023; Sepúlveda and Padilla, 2008), largely due to the complex nature of volcanic soils and their marked textural variability (Thompson et al., 2023), which strongly influence water retention and infiltration dynamics. Recurrent debris flows in the Osorno volcano exemplify the role of intense rainfall events and the mobilization of autobrecciated lava blocks in

initiating such processes (Fustos-Toribio et al., 2022). Although numerical modeling has estimated total flow volumes (ranging from 4.7×10^5 to $5.5 \times 10^5 \text{ m}^3$) highlighting the high sensitivity of debris flow generation to the initial water content, a comprehensive conceptual model remains lacking. Over the past four decades, the Southern Andes has experienced significant volcanic activity (Galletto et al., 2023), resulting in widespread tephra deposition that has contributed to increased frequencies of debris flows (Korup et al., 2019). Nevertheless, critical knowledge gaps persist regarding the spatial and temporal variability of the textural and hydraulic properties of volcanic soils, particularly under extreme hydrometeorological conditions. Addressing these gaps is crucial to better constrain the hydraulic and geomechanical conditions that lead to debris flow initiation (Schmidt et al., 2001; Kuriakose et al., 2009). Such understanding is fundamental for effective territorial planning, risk mitigation, and the development of robust early warning systems.

In this paper, we analyse the precursory surface deformation related to tensile cracks leading to the Ñisoleufu debris flow event (31 May 2021). We utilised a multi-temporal InSAR approach with Sentinel-1 C-band SAR data, enabling us to create time series plots of deformation before the landslide and compare them with available daily precipitation records from nearby weather stations and satellite measurements. By combining remote sensing data, weather records, and soil laboratory analyses, we aim to provide valuable insights into the factors leading to such events and, consequently, improve hazard assessment and management in zones with soils derived from explosive volcanic events.

2 Study area

Debris flows are the most common manifestation of mass wasting triggered by precipitation in the Southern Andes due to the soil heterogeneity and geological features, providing a unique opportunity to study the relationship between extreme rainfall and debris flows (Fig. 1A–D). Recent extreme precipitation events have produced mass wasting hazard, especially in steep zones near alluvial plains where human settlements are often established (Fustos et al., 2017; Fustos-Toribio et al., 2021). On 31 May 2021, a very fast debris flow was triggered due to extreme rainfall affecting houses and blocking the CH-201 route in the Ñisoleufu zone, southern Chile, generating economic losses in a vulnerable rural area (Figs. 1B, 2). The deposit mainly consisted of rock blocks and trunks covered by a thin layer of debris. Much of the debris flow fell into the adjacent Calafquén lake (Fig. 2), causing a small tsunami. The event was extremely rapid, based on the classification proposed by Hungr et al. (2014), with a speed estimated to be over 3 m s^{-1} . Stand out that the debris flow experienced reactivation events on 19 June 2023, and again on 28 June 2024.

The debris flow was deposited in a flat area of the valley (slopes between 0 and 20°), flowing into Lake Calafquén. The presence of landslide deposits and old flows in the vicinity of the lake (Fig. 2A; geologic map [Ha]) suggests that this phenomenon is common in the area.

The Ñisoleufu area exhibits a geological sequence (Fig. 2A) starting at the base with the Futrono-Riñihue Batholith (CPgfr), followed by stratified volcano-sedimentary units (Pliv) and topped by glacial deposits (Plm2). Within this sequence, the Sierra Quinchilca volcano-sedimentary unit has been dated to less than 1 million years and is in nonconformity contact with the underlying rocks of the Futrono-Riñihue Batholith. Consolidated glacial deposits from the last glacial maximum period show variable depths, ranging from 1 m to 10 cm, and lie in erosive unconformity over the volcano-sedimentary units (Pliv). The area also exhibits mass movement deposits (Hrm and Ha) covering the older units on the north slope of Sierra Quinchilca (Pliv, Fig. 2A; Rodríguez et al., 1999).

3 Methodology

To assess the triggering and conditioning factors in glacial environments in Southern Andes, we assessed in detail the Ñisoleufu debris flow (Fig. 3). To achieve this, we employed two complementary methodologies. The first methodology involved fieldwork, including soil sampling and subsequent laboratory analysis to evaluate the geotechnical features influencing debris flow initiation. The second methodology utilized numerical models to analyse meteorological conditions in the study area, such as precipitation patterns, variations in soil moisture, and landforms associated with erosion and deposition zones linked to the landslide. This endeavour involved a meticulous examination of the rheological and hydraulic attributes of the soil, facilitating an understanding of past and contemporary surface processes. Through this analytical framework, it became feasible to discern causative factors contributing to the event, thereby enabling an informed evaluation of the potential risk posed by analogous occurrences in the future.

3.1 Geomorphological and geotechnical conditions

To analyse the geomorphological characteristics of the area, we utilised a 12.5 m resolution ALOS PALSAR DEM data, from which slope, aspect, and elevation maps were derived. A terrestrial and remote sensing survey was carried out to characterise the physiography of the hillslope before and after the debris flow. We employed the Normalized Difference Vegetation Index (NDVI) to delineate the area affected by the debris flow. We calculated the NDVI using two Sentinel-2 acquisitions on 13 May and 14 June 2021, corresponding to the Ñisoleufu debris-flow event on 31 May 2021. Field campaigns were conducted 1 d and 3 months after the event

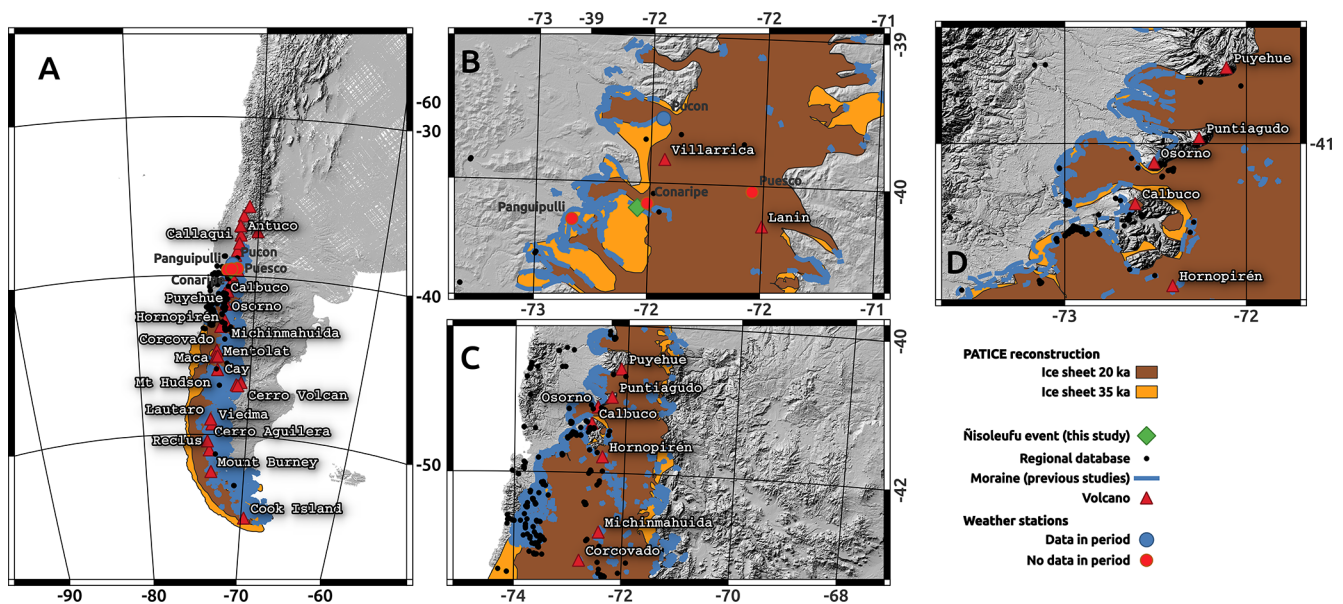


Figure 1. Rainfall-Induced mass wasting in Southern Andes. (A) Regional map of Ice-sheet extension during 35 and 20 ka as example and volcanoes emplaced in the area. (B) Zoom to study area with Ñisoleufu in Northern Ice sheet sector showing the weather stations. (C) Zoom to Northern Patagonian area showing correlation between mass wasting events and moraine lines (blue line). (D) Zoom to Osorno volcano area showing high debris flow generation area discussed in Fustos-Toribio et al. (2022).

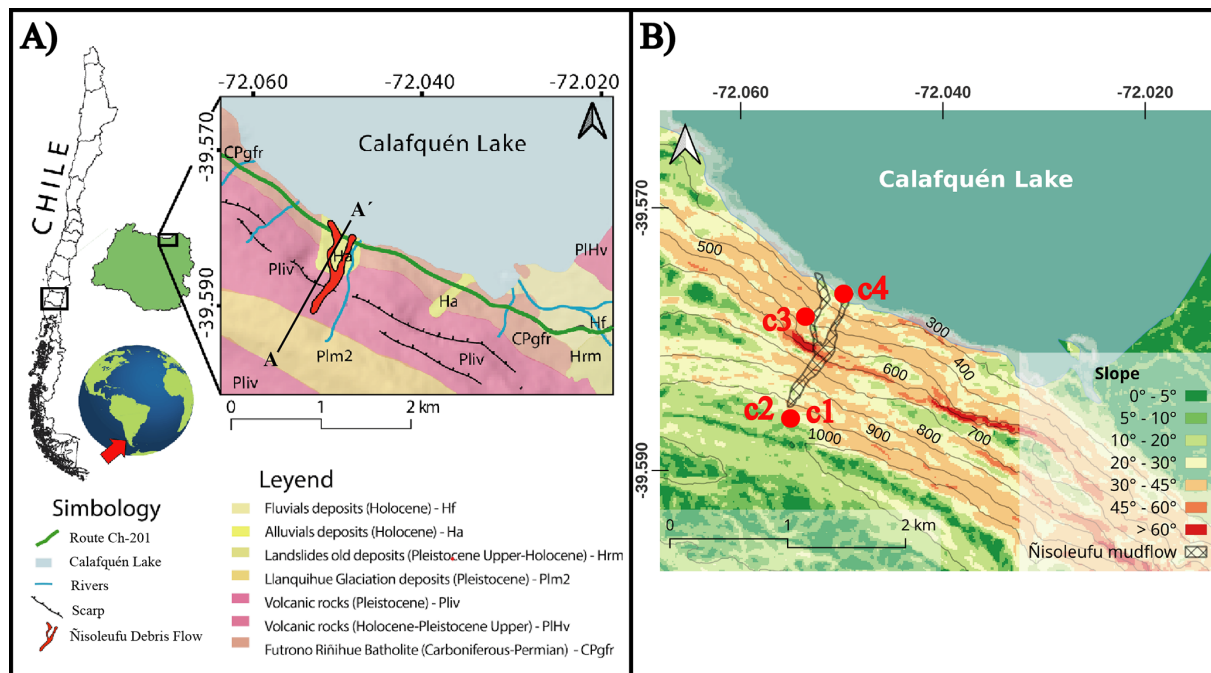


Figure 2. (A) Geological map of area study based on Rodriguez et al. (1999). (B) Slope and elevation values (m a.s.l.).

(1 June and September 2021) to characterise post-event geomorphological features. Field observations were determinant in the identification of the sediment budget of the channel, aiding the assessment of the event's characteristics (a channelised, stony debris flow) and the movement dynam-

ics in the hillslope. On-channel deposits were assessed using cross-sections along the Ñisoleufu sector. Peak flow marks were documented, and erosion depths were estimated based on erosion marks and bedrock exposures over three cross-sections.

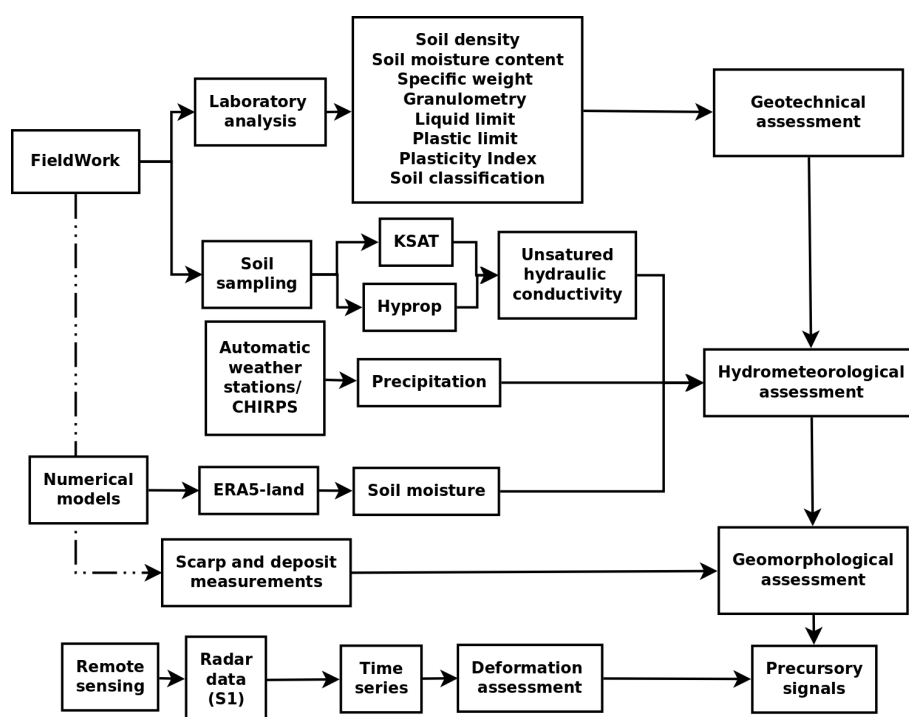


Figure 3. Methodological approach.

Moreover, an exhaustive analysis of the geomorphological changes resulting from the event was conducted. A detailed survey of the stratigraphic column was conducted at three key points (Points c1, c2 and c4 in Fig. 2B). Firstly, a stratigraphy sequence at the base of the debris flow was generated, obtaining the deposit sequence and assessing previous non-documented events. Secondly, a survey was conducted in the headscarp area where the event was initiated, evaluating the geological and geomorphological conditions that led to its generation. This approach allowed for the characterisation of the strata and structures in the affected area, seeking insights into the triggering mechanisms of the flow. Additionally, a detailed evaluation of the lateral erosion caused by the flow was carried out to understand the impact of local geomorphological changes as proxies for similar glacial-volcanic environments (Bucher et al., 2024). Finally, we assessed changes in vegetation that occurred as a result of the 31 May event and its subsequent reactivations (Fig. 2B), allowing the estimation of the evolution of the landscape.

To analyse the geotechnical features that support a debris flow generation or another type of mass wasting antecedent, soil samples were collected in the generation zone. We determined soil density (ρ) following the UNE 103-301-94, soil moisture content (NCh 1515), specific weight (ASTM D854-14) standards. Granulometry analysis was carried out using sieve and hydrometer methods based on Kinde et al. (2024). The liquid limit was determined using AS 1289.3.9.1, and the plastic limit was evaluated following NCh 1517/2 standard, allowing to obtain the Plasticity Index. Finally, the soils were

classified based on ASTM D2487-17. These comprehensive geotechnical analyses provided crucial insights into the soil properties and their potential role in the occurrence of the debris flow event.

3.2 Hydrometeorological conditions

To analyse the hydrometeorological conditions, we investigate the influence of rainfall in the study area, analysing hourly/daily data from four weather stations (Fig. 1B) from the INIA agrometeorological and DMC networks (<https://agrometeorologia.cl/>, last access: 25 November 2025) and the Climate Hazards Group InfraRed Precipitation with Station (CHIRPS) precipitation estimates (Funk et al., 2015). Soil moisture data from the ERA5-land product was utilised to complement the analysis considering the antecedent soil moisture at different depths before debris flow (Bordoni et al., 2023; Palazzolo et al., 2023), being considered suitable due to their accurate soil moisture data in hydrological cases (Muñoz-Sabater et al., 2021). The ERA5 product provides valuable and reliable information on soil moisture, enabling a more comprehensive understanding of the hydrological conditions that could trigger debris flows in the area. To understand the water transfer capacity along the soil, we measured the layer thicknesses from visual assessment of the soil profile in the scar (Fig. 4). We followed the experimental design of De Pue et al. (2019) considering two samples per layer. One sample was used to measure the soil moisture ($\Theta(h)$) and unsaturated hydraulic conductivity (K_u) using the evapo-

ration method (HYPROP[®], Meter Group), meanwhile, saturated hydraulic conductivity K_s was measured using KSAT[®] equipment (Meter Group), using the falling head method (Dane and Clarke Topp, 2002). The hydraulic conductivity will provide valuable information about the layer's ability to allow water to flow through, which could have played a significant role in the initiation and propagation of the debris flow.

3.3 Remote sensing and precursory signals

We assessed precursory signals estimating surface deformation by the Stanford Method for Persistent Scatterers (StaMPS; Hooper et al., 2007, 2012) using Sentinel-1 C-band SAR data. We downloaded 35 ascending orbit (track 164) and 18 descending orbit (track 83) Sentinel-1 images covering the period from November 2020 to June 2021, which includes 7 months before the 31 May debris flow in the Ñisoleufu sector (Table 1). We also included two acquisitions after the debris flow in both orbits to analyse the slope's response to non-rainfall and rainfall periods. Initially, we analysed data until the end of July, but snow coverage led to coherence loss in the area, resulting in a low density of Persistent Scatterer points (PS points) per km². Consequently, we evaluated different combinations of bands from Sentinel-2 images (based on bands 4, 3, 2) to assess the maximum amount of SAR images available before the snow period. This approach allowed us to optimise the data selection process and continue our analysis effectively.

The SAR data was processed using open-source Sentinel Application Platform (SNAP) packages through the snap2stamps routines, enabling us to generate single-master interferograms compatible with StaMPS. Further details on the snap2stamps routine in Fomelis et al. (2018) and Blasco and Fomeli (2018). First, the initial selection of PS points is performed based on their noise characteristics, using the amplitude dispersion criterion, which is defined by $D_{\text{Amp}} = \sigma_{\text{Amp}}/m_{\text{Amp}}$, where σ_{Amp} and m_{Amp} are the standard deviation and mean of the amplitude in time, respectively (Ferretti et al., 2001). We selected a threshold value of 0.4 for D_{Amp} as a typical threshold value (Hooper et al., 2007), and subsequently, some initial parameters were modified according to the values proposed by Höser (2018). This allowed us to plot surface soil deformation using time series, which we then compared with daily precipitation records obtained from nearby weather stations and satellite measurements. Lastly, we used the GACOS correction (Yu et al., 2018) through the TRAIN toolbox (Bekaert et al., 2015) to reduce the atmospheric phase component. We complemented surface deformation with antecedent precipitation to establish precursory signals and their correlation with precipitation. We calculated the accumulated precipitation between the dates of the SAR acquisitions and the total accumulated precipitation for the entire period. We assessed daily precipitation and their temporal changes to understand the antecedent pre-

cipitation in the debris flow event. The four weather stations were identified within a reasonable radius for potential use as sources of meteorological data. However, upon examining the temporal coverage and continuity of their records, it was found that only the Pucón station had complete and operational data for the study period. Moreover, we merged this data with CHIRPS dataset for comparison with the time series of deformation to examine the relationship between precipitation and deformation.

4 Results

4.1 Geomorphological and geotechnical conditions

The extension of the area affected by the debris flow was evaluated, identifying and characterizing the triggering conditions (Fig. 5A). The results revealed significant differences in the Normalized Difference Vegetation Index (NDVI), which facilitated the delimitation of the landslide area (Fig. 5A). Low positive NDVI values (< 0.20) are shown for the area affected by the debris flow, encompassing 118 575 m², in contrast to the normally high NDVI values (0.6–0.8) of surrounding areas. The debris flow moved along a complex and abrupt geometry, with slopes varying from 20° near the ridges (950 m a.s.l.) and the base of the slope (250 m a.s.l.), to almost vertical areas ($\sim 90^\circ$) in the intermediate zone (550 m a.s.l.) (Figs. 4a and 5D). This geomorphological configuration is typical of glacially eroded valleys (U-shaped valleys) in the southern Andes, a recurrent phenomenon in the formation of valleys at this latitude (Muratli et al., 2010).

The initial landslide crown has an altitude of 950 m a.s.l. and slopes of approximately 20 to 30° (column c1 in Fig. 5D). The flow release zone (inset C in Fig. 4) has evidence of extensional failures, where c1 indicates that the first level S-1 corresponds to a very compact chaotic and polymictic till deposit (Plm2), with a greyish matrix containing a higher percentage of clay than sand. Some clasts exceed 10 cm and are composed of volcanic fragments (Pliv), as well as intrusive material (CPfgr). Towards the top of the glacial deposit, level S-2 is observed, a thin, grey fluvioglacial deposit (varves), approximately 40 cm thick, composed of a well-consolidated matrix of clay-rich (dark) and silt-rich (light) setting a couplet annual sediment layer (Figs. 4b and 5D). Above the glacial deposit, level S-4 is identified, composed mainly of lapilli-sized deposits (> 5 mm), associated with pumice from the Neltume deposit of the Mocho-Choshuenco Volcanic Complex, dating $10\,200 \pm 500$ BP (Rawson et al., 2015; Moreno-Yaeger et al., 2024). Finally, level S-7 corresponds to the current soil where native forest develops (Fig. 4a, c).

Stratigraphic analysis along the slope (Fig. 5B–D) reveals a consistent sequence overlying the CPfgr basement, characterized by a basal glacial deposit (S-1) with large an-

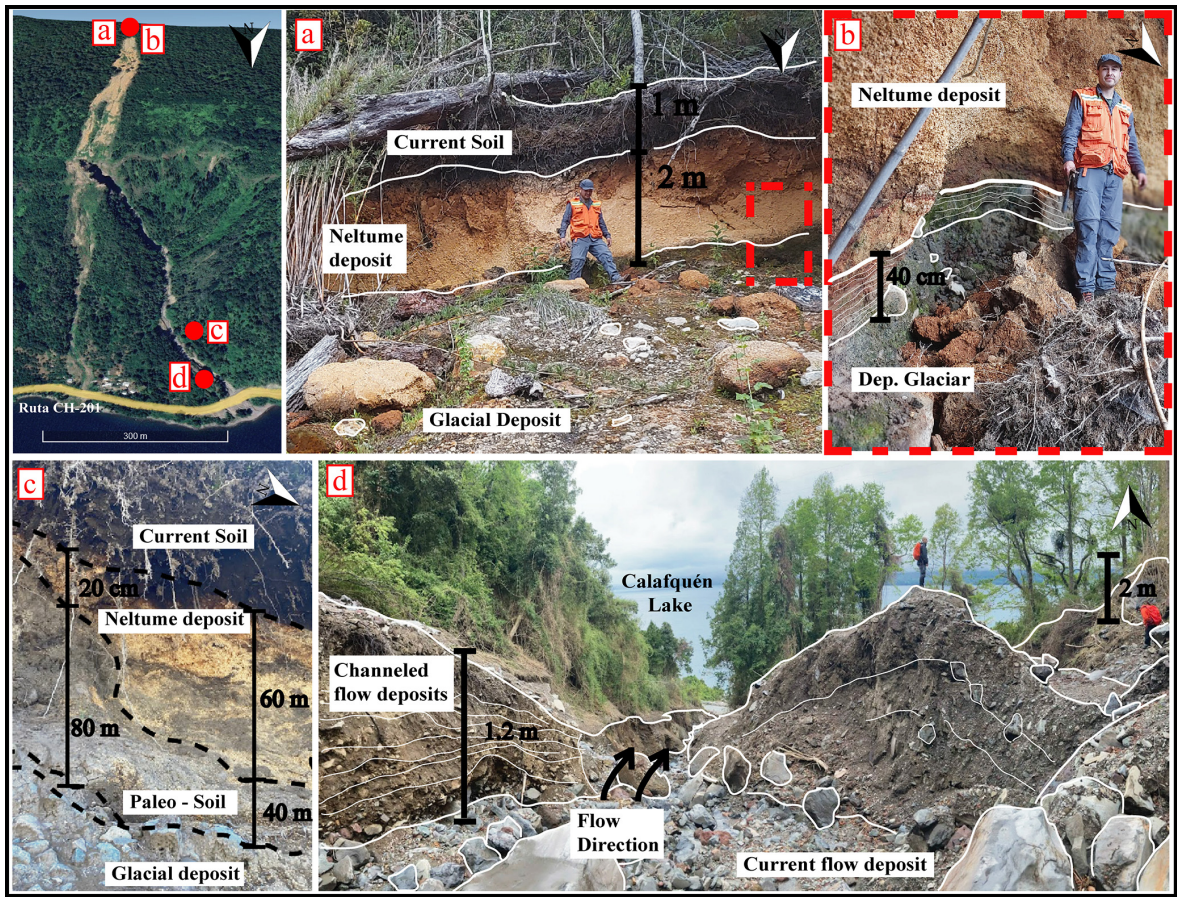


Figure 4. Field photographs indicating soil deposits in scarp (a, b) and the deposits in the toe (inset c and d).

Table 1. Data used in temporal analysis using SAR data.

	Track	Frame	First Image	Last Image	Total Images	Primary Image	Sub-Swath
DES	83	93	2 November 2020	18 June 2021	18	2 March 2021	IW2
ASC	164	1048	1 November 2020	17 June 2021	35	11 February 2021	IW3

gular clasts, overlain by silt–clay layers (S-2). These low-permeability units are covered by interbedded paleosols and volcanic ash-falls. In column c3, the paleosol S-3 was initially considered older than the Neltume ashfall, but the presence of reworked pyroclasts in S-4 (Fig. 4d) suggests a younger relative age. The upper sequence concludes with active soil formation (S-7; Figs. 4a, c, 5D). Further downslope (250 m a.s.l.), column c4 exhibits a distinct stratigraphy dominated by mass-wasting deposits. The basal level (S-5) consists of a polymictic unit with sub-rounded clasts and pumice fragments from the Neltume event, embedded in a clay-rich matrix derived from upstream glacial units. A similar, though finer, deposit (S-6) overlies S-5, and is capped by the same modern soil unit (S-7). This stratigraphic framework – composed of alternating low-permeability substrates and reworked tephras – is represen-

tative of Andean terrains between 39 and 42° S and is critical to understanding hydrological storage and slope instability (Fig. 1). From a geotechnical perspective, the first soil (S-2) has a liquid limit of 27.48 and a plastic limit of 16.07, resulting in a plasticity index of 11. This soil exhibits a low plasticity and is classified as a silt (CL) according to the Unified Soil Classification System (USCS). S-3 showed a liquid limit of 123.93 and a plastic limit of 91.3, resulting in a plasticity index of 33. This soil exhibits a moderate plasticity and is classified as a plastic silt (CH), according to the USCS. Meanwhile, S-7 has a liquid limit of 149.83 and a plastic limit of 114.13, resulting in a plasticity index of 36, showing a high plasticity and is classified as a plastic organic soil (OH). The granulometric analysis (Fig. 6; S-3 and S-7) confirms this classification, with silt and sand content between 70 % and 90 %. Due to

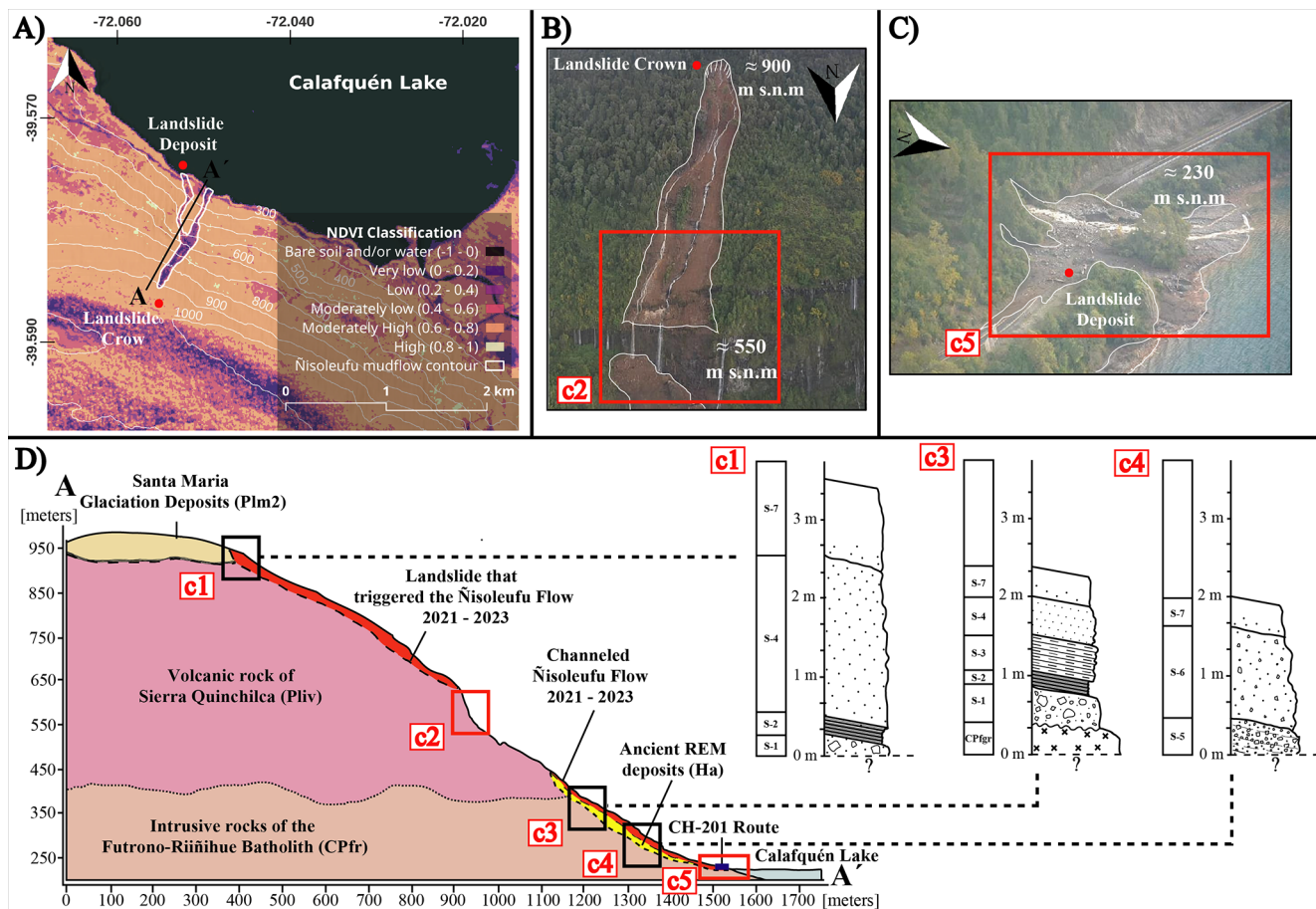


Figure 5. (A) Normalized Difference Vegetation Index (NDVI) highlighting the erosive zone generated by the Ñisoleufu debris flow. (B, C) Photos taken by a drone on 1 June 2021, highlighting the crown of the debris-flow (B), and the landslide deposit and the development of many waterfalls around the flow in red (C). (D) Profile of the sequence where the flow occurred and stratigraphic columns. Photos: Carrasco and Ramírez (2021).

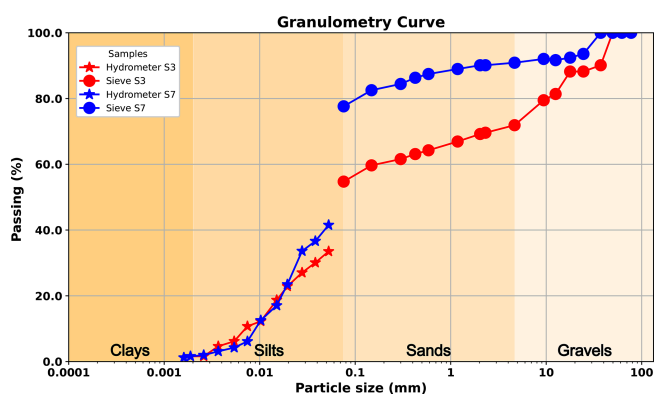


Figure 6. Soil granulometric curve of S-3 and S-7.

the soil properties, S-4 (Neltume ashfall pyroclastic) has not been characterised in the laboratory due to the high fragility of the pyroclasts classified as lapilli ($\varnothing > 5$ mm) being too coarse to measure their limits.

4.2 Hydrometeorological conditions and precursory signals

The debris flow release zone (Figs. 4a, 5B and column c1 in Fig. 5D) provided accurate soil measurements using KSAT, enabling us to understand the factors governing water transport on the slope. Field mapping revealed a layered model that identified a highly stratified environment with distinct characteristics (Figs. 4b; 7). It was observed that the glacial deposits underlying layers of volcanic origin regulate water movement in the soil due to their low hydraulic conductivity (Fig. 7). These glacial deposits, identified as moraines and varves, are associated with the Last Glacial Maximum (LGM), correlated with nearby deposits and natural terrain conditions.

Notably, volcanic soil deposits (Fig. 6; granular texture description) and Neltume ashfall demonstrating high saturated hydraulic conductivity of 4.64×10^{-5} to $3.31 \times 10^{-4} \text{ m s}^{-1}$ (Fig. 7). This characteristic is critical as it facilitates the movement of infiltrated water from the organic surface

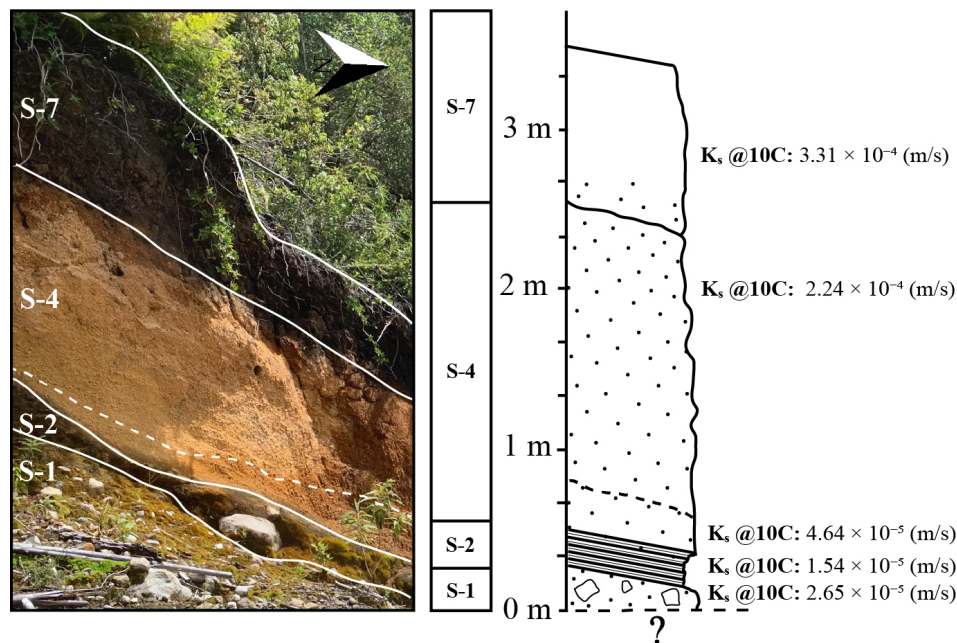


Figure 7. Hydraulic properties of release zone in debris flow generation zone (column c1 in Fig. 5D).

to the slope's interior. In contrast, Varves-type glacial deposits show low hydraulic conductivity, with values of $1.54 \times 10^{-5} \text{ m s}^{-1}$, while the till reached a K_s of $2.65 \times 10^{-5} \text{ m s}^{-1}$, both acting as partial barriers to water movement. Nevertheless, their storage capacity is significant, particularly when situated on moraines that, due to their varied granulometric distribution, retain water effectively. The hydraulic conductivity and the high infiltration rate derived from the Porchet test showed a moderately high infiltrated rate (112.70 mm h^{-1}), computing a $k = 3.31 \times 10^{-4} \text{ (m s}^{-1}\text{)}$ in the superior organic deposit layer (S-7; Table 2 and Fig. 7).

Analysis using the ERA5 model reveals a well-defined annual cycle in soil moisture (Fig. 8A). While the overall evolution of moisture content does not indicate an anomalous trend when compared to previous years, significant short-term variations in soil moisture were observed (Fig. 8B) in response to extreme precipitation events (Fig. 8C). The preliminary results showed that antecedent rainfall led to surface saturation, with moisture levels reaching full saturation within the first metre of soil depth, primarily due to accumulated rainfall in the days prior (Fig. 8B–C). Notably, a substantial and rapid increase in soil moisture was also detected at greater depths – up to 2.89 m – where a 50 % change occurred shortly before the onset of debris flow events (Fig. 8B). This marked fluctuation was concentrated at the interface between tephra and till-varves, suggesting critical implications for slope instability. Our findings underscore that, even in the absence of a long-term anomalous trend, the combination of saturated soil conditions and intense rainfall plays a decisive role in triggering debris flows.

The availability of a sufficient quantity of SAR images and the revisit times of Sentinel-1 enabled a well-distributed temporal analysis of slope behaviour before the debris-flow event on 31 May 2021. We measured surface deformation between $+9$ and -32 mm yr^{-1} . The results of PS estimation suggest the occurrence of surface subsidence consistent change in soil water content (Fig. 8B). Our analysis reveals a precursory deformation signal that comprised two distinct phases (Fig. 9). The first phase, beginning in late January 2021 and extending through April, exhibited a high-deformation pattern associated with consistent precipitation (Fig. 8C), which infiltrated the soil and increased soil moisture levels (Fig. 8B). This timing coincides with a significant precipitation event in late January, suggesting that summer rainfall may have acted as an initial trigger, initiating a surface deformation that evolved progressively over time. A second deformation phase following a high-intensity rainfall event in mid-to-late May 2021, characterized by pre-event deformation patterns. Despite that most evident precipitation event occurred in late May (15 d before), our surface deformation estimations could suggest that the triggering process likely began approximately in summer period. This temporal relationship between precipitation and deformation further underscores the need for incorporating hydrological factors into models of surface stability and landslide risk assessment. Finally, the deformation measurements are interrupted a few days before the debris flow occurs. This data interruption is attributed to the formation of significant extensional fractures (Fig. 4d–e), causing a loss of coherence in the data (red box).

Table 2. Physical properties of soils related to the column c3.

Soil type/Property	Normative	S-2	S-3	S-4	S-7
Moisture [w] (%)	NCh-1515	17.8	56.2	119.3	111.6
Density [ρ] (g cm ¹³)	UNE-103-301-94	2.07	1.52	< 1	1.06
Specific Gravity [G_s]	ASTM-D854-14	2.76	2.49	2.5	2.34
Liquid Limit [W_L] (%)	AS 1289.3.9.1	27.48	123.93	–	149.83
Plastic Limit [W_p] (%)	Nch 1517/2	16.07	91.3	–	114.13
Plasticity Index [PL]	NCh1517/2	11	33	–	36
Hydraulic Conductivity [k_u] (m s ^{−1})	Porchet and Laferriere (1935)	–	–	–	3.13×10^{-4}

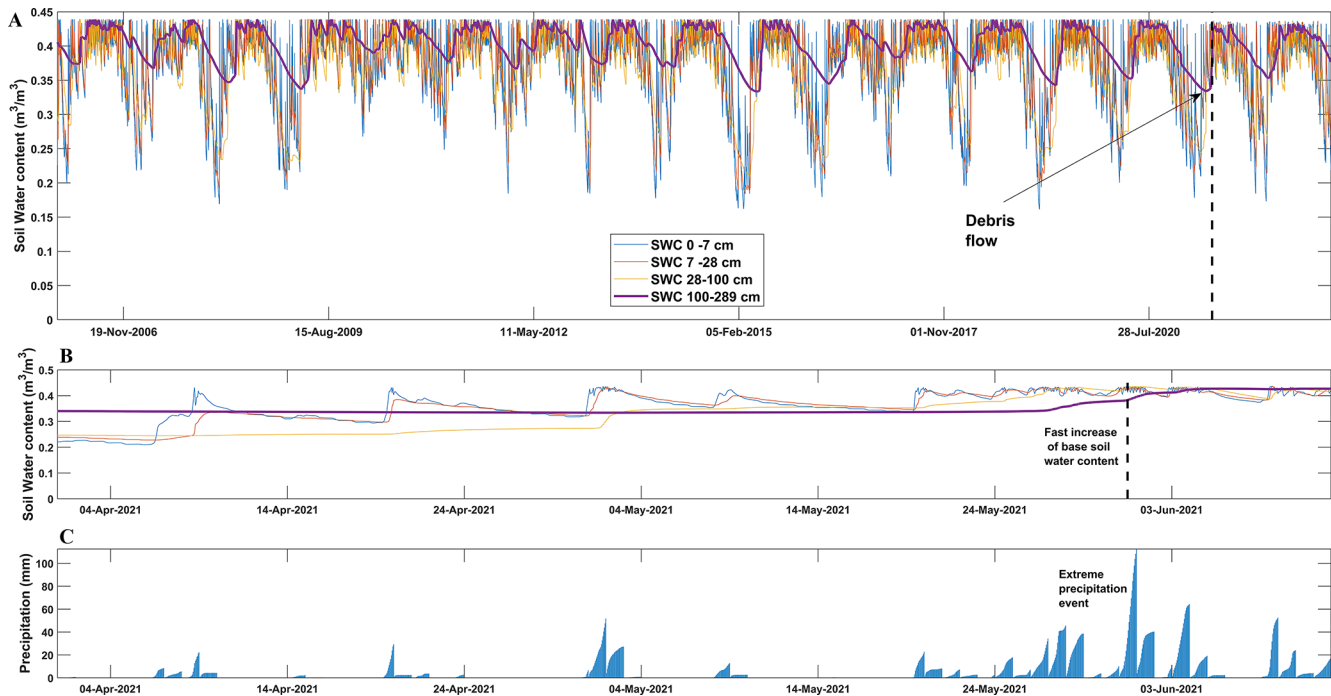


Figure 8. Assessment of ERA5-land product over debris flow generation. (A) Assessment of time series of soil moisture at different depths. (B) Zoom to Soil moisture weeks previous to debris flow. (C) Rainfall events accumulated at 24-hourly scale (ERA5-land).

5 Discussion

To improve debris-flow hazard assessment, it is crucial to understand how multiple controlling factors converge to trigger these events. In the Ñisoleufu case, we studied the triggering conditions of debris flow in an area to understand precursory signals of mass wasting initiation in post glacial and volcanic environments. We considered a geomorphological, geotechnical, hydrometeorological and surface deformation approach to constraint the variability of the mass wasting processes in one representative area of the Southern Andes.

5.1 Geomorphological and geotechnical implications

The occurrence of mass wasting events, such as landslides and debris flows, following periods of intense rainfall has been extensively studied in the Southern Andes using lo-

cal cases, mainly based on the rainfall control over the mass wasting generation (Fustos et al., 2020b; Maragaño-Carmona et al., 2023) without consider the soil features as noted recently (Vásquez-Antipán et al., 2025). Our results showed that the geomorphology plays a crucial role in the generation of debris flows, particularly through its influence on water accumulation in catchment areas, such as micro-basins (Fustos-Toribio et al., 2021). We considered two main geomorphological controls for debris flow initiation. First, stand out the steep slope ($> 45^\circ$), which was a significant contributing factor to the generation of the Ñisoleufu debris flow (Figs. 2 and 5B–D). Second, the northern orientation of the slope could also be a relevant factor, as in the central-southern Chile domain ($36\text{--}42^\circ\text{ S}$), atmospheric moist flux from extreme rainfall tends to flow in a northwest (NW) direction, with orographic forcing triggering being enhanced by the Andean belt (Valenzuela and Garreaud, 2019;

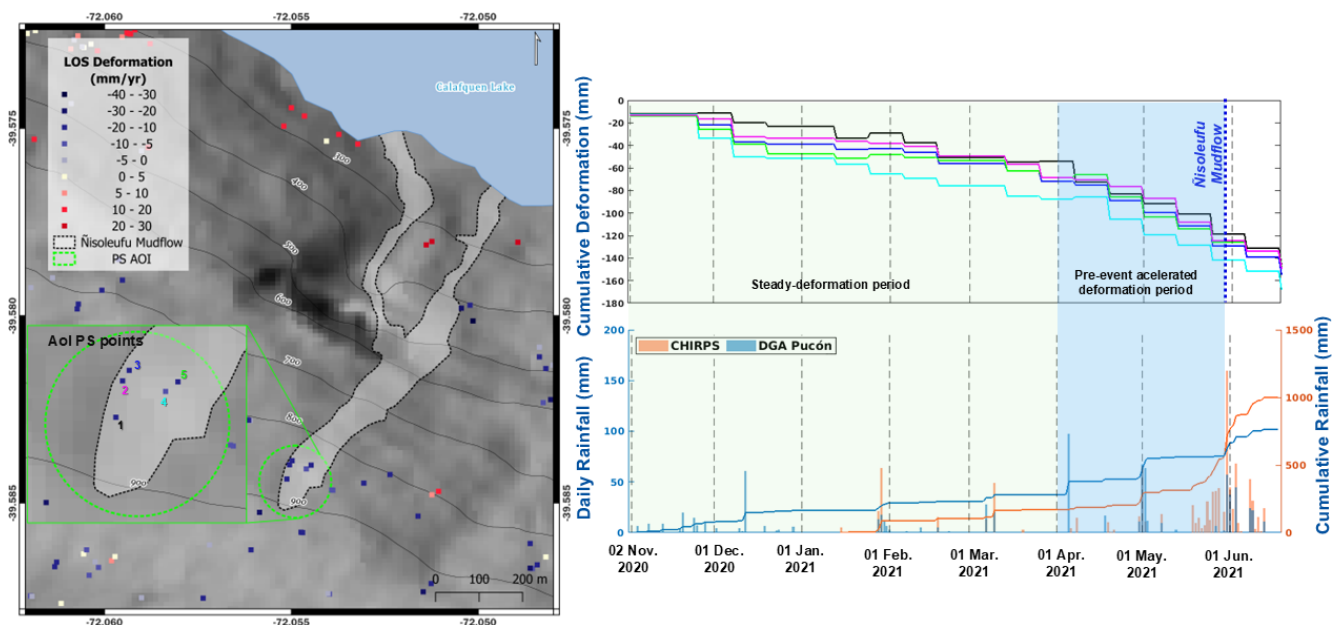


Figure 9. points obtained with Sentinel-1 “ascending” orbit data before debris flow initiation. Precipitation time series using Pucón weather station. Deformation shows an subsidence in surface.

Vásquez-Antipán et al., 2025). The interplay between areas with high water accumulation capacity from local runoff and the slope’s propensity to capture precipitation was instrumental in the generation of the debris flow. Stand out the slope that facilitated an efficient surface drainage of water from higher areas, leading to the formation of local accumulation and infiltration zones that promote the build-up of subsurface pore-water pressures (Fig. 8B) leading to the debris flow event, facilitating a rapid downslope movement of soil once it became saturated.

The geotechnical stability of soils in the Southern Andes, could be controlled by the interaction between explosive volcanic. Mocho-Choshuenco volcanic complex (MCVC) and glacial processes and the resultant varved deposits (Figs. 4b, 7) has been modulated the slope stability around the 39° S. The Neltume ashfall deposit related to the eruption of the MCVC ($10\,200 \pm 500$ BP; Rawson et al., 2015) played a significant role in the formation of the S-4 (Fig. 4a–c). The thickness of all soils varies along the scar left by the debris flow, with the magnitude strongly influenced by the topographic gradient and/or erosion processes that might have occurred and following reworking (Fig. 4c). Moreover, glacial deposit like as varves, formed from sedimentation during glacial periods, played a crucial role in the soil’s physical and mechanical properties controlling the area with low hydraulic conductivity (Fig. 7) introducing a water barrier in the area to regional scale.

Moreover, field evidence suggests that the Ñisoleufu event is not an isolated case, as indicated by other remobilised events in the area (Fig. 2, geological map – alluvial deposit: Ha). The geotechnical properties of the remobilised materi-

als are critical for defining slope stability conditions. Granulometric analyses indicate that the deposits are primarily granular soils, such as those associated with S-4, which are classified as frictional and are found overlying finer-grained cohesive soils, such as varves (S-2). Other soils found in the Southern Andes, including S-3 and S-7, originate from the decomposition of volcanic glass and glacial clays (Sanhueza et al., 2011; Vásquez-Antipán et al., 2025), producing particles smaller than 0.1 mm (Fig. 6).

Specifically, S-3 soils, derived from explosive eruptions of the Mocho-Choshuenco volcano, consist of non-cohesive volcanic ash mixed with fine-grained sediments, forming a matrix with elevated plasticity and a high liquid limit (Vásquez-Antipán et al., 2025). These properties result from the introduction of fine material during the deposition. Moreover, S-7 soils, classified as organic soils derived from volcanic deposits, exhibit notably high liquid limits due to the accumulation of organic matter. The organic matter enhances the soil’s water retention and promotes the formation of organic colloids, which may increase the liquid limit (Deng et al., 2017; Fiantis et al., 2019). Our results are consistent with independent laboratory testing in the zone (Vásquez-Antipán et al., 2025), which shows that organic-rich paleosols were buried after the Last Glacial Maximum, approximately 5 km south of the study area, and exhibit similar liquid limit values to those observed in S-7.

The spatial distribution of soil layers varies abruptly along the slope, as observed in columns c1 and c3 for S-1, S-2, and S-4, indicating significant mass wasting and erosion processes near glacial lakes (Fig. 5D). The frictional soils, such as those related to S-4, generally exhibit high shear strength

(Chen et al., 2021), and when combined with steep topography, may contribute to the relative stability of post-glacial volcanic deposits (Walding et al., 2023; Ontiveros-Ortega et al., 2023). However, under extreme precipitation events – such as those recorded in recent years in the Southern Andes – soil saturation can substantially reduce the strength of even frictional soils, increasing the likelihood of failure (Fustos et al., 2017; Somos-Valenzuela et al., 2020; Fustos-Toribio et al., 2021). This mechanism aligns with the observed extensional failures that preceded the initiation and reactivation of flows in June 2023 and 2024 (Figs. 4b; 10).

We propose that the event of Ñisoleufu, a classical case of the Southern Andes, was triggered by the soil saturation, reducing the effective stress within the soil matrix leading to extensional failure in the volcanic deposits (Figs. 4b; 10), highlighting the risks associated with this saturation, particularly in areas where explosive volcanic activity has previously occurred, leading to increased susceptibility to debris flows and other forms of mass wasting (Korup et al., 2019). The interaction between glacial deposits and volcanic materials creates a unique geotechnical environment where the stability of slopes is contingent upon both the physical properties of the soil and the hydrological conditions present.

5.2 Hydrometeorological conditions and precursory signals implications

The volcanic origin and composition of the soils evidenced a high soil moisture variability along the year. ERA5-land data reveals a sudden change in soil moisture content at various depths on the base of the debris flow initiation supporting the surface deformation days before the landslide (Fig. 9). The water role in the event proposes that accumulation of subsurface water in granular soil could serve as a storage medium. The fine media of S-1 and S-2, with its low hydraulic conductivity, acts as barrier layer, enhancing the storage capacity of S-4 in the crown of the debris flow. This is supported by the hydraulic properties of S-3 (CH) and S-7 (OH), combined with Porchet's study on the current soil (S-7: 112.70 mm h^{-1}), which indicates a moderately high infiltration rate and suggests high hydraulic conductivity for the Ñisoleufu soils (Fig. 7). The combination of these factors contributes to the overall permeability of the volcanic soils, a main feature in the Southern Andes, potentially influencing water movement and retention in the area.

The water storage is consistent with surface deformation data, reaching -85 mm yr^{-1} in the previous 30 d of the event, offering insights of previous surface deformation to the occurrence of debris flow events in areas where glacial deposits and volcanic deposits coexist (Fig. 9). The atypical nature of these deformations suggests that the surface shows a slow movement related to subsidence along LOS, followed by the debris-flow event on 31 May 2021 (159.8 mm yr^{-1}). The constant slope deformation supports the hypothesis of the development of extensional failure, ultimately resulting

in the observed a small landslide and subsequent release of water as debris flows (insets d and e in Fig. 10).

The fast saturation of S-4 is exacerbated by increased water availability due to rainfall and by the presence of a bottom layer with low hydraulic conductivity associated with fine soils (S-2), being a common denominator in the Southern Andes. S-2 retains water and further reduces the shear strength of the underlying granular soil. Additionally, these soils could act as lubricants, reducing the overall slope shear strength. The interaction between glacial deposits and explosive volcanic eruption deposits in the cordilleran zone of the Southern Andes creates a scenario prone to slope deformation and mass removal, especially debris flow. Our results suggest that the combination of geological and climatic factors in this region generates ideal conditions for the occurrence of mass removal events under extreme precipitation events (Savi et al., 2016).

Our results showed a limited amount of PS in the study area similar to previous studies in the area (Vásquez-Antipán et al., 2025). The Southern Andes, and the Ñisoleufu area, is characterized by complex geomorphological features and varying precipitation patterns that could introduce uncertainty to the remote sensing measurements. The application of limited persistent scatterer data in assessing slope deformations offers a promising avenue for the development of a landslide early warning system (LEWS) in the Southern Andes. However, the investigation into this method requires a thorough understanding of potential limitations, particularly the extensive vegetation cover in the Southern Andes, which can obscure satellite signals and affect data accuracy. Vegetation serves as a significant barrier to radar signals, leading to incomplete datasets that might obscure important geological signals indicative of slope movements (Maragaño-Carmona et al., 2023). Therefore, additional efforts must be considered to move forward to an operational scale.

Climate change is increasingly debris flow generation by altering precipitation patterns and soil moisture dynamics (Talebi et al., 2007). In the Southern Andes, volcanic soils with variable textures play a critical role in this process. Enhanced seasonal moisture variability, exacerbated by extreme precipitation, leads to fast soil saturation, especially where fine-grained soils form low-permeability layers above coarser materials (Fig. 10). These stratified soil conditions promote subsurface water storage, increasing the slope instability under saturated conditions (Talebi et al., 2007). Fine volcanic over glacial deposits can act as lubricants, further weakening slope cohesion and promoting failure (Kameda et al., 2019) during intense rainfall, as happened during the Ñisoleufu event (Fig. 10). This event highlights how short-duration storms, increasingly associated with climate change, can overwhelm the buffering capacity of mountainous terrain. The soil media S-7 and S-4, both composed of organic-rich and granular volcanic materials, played a critical role in this response. During the 2023 event, infiltrating rainwater rapidly percolated through these coarse upper layers

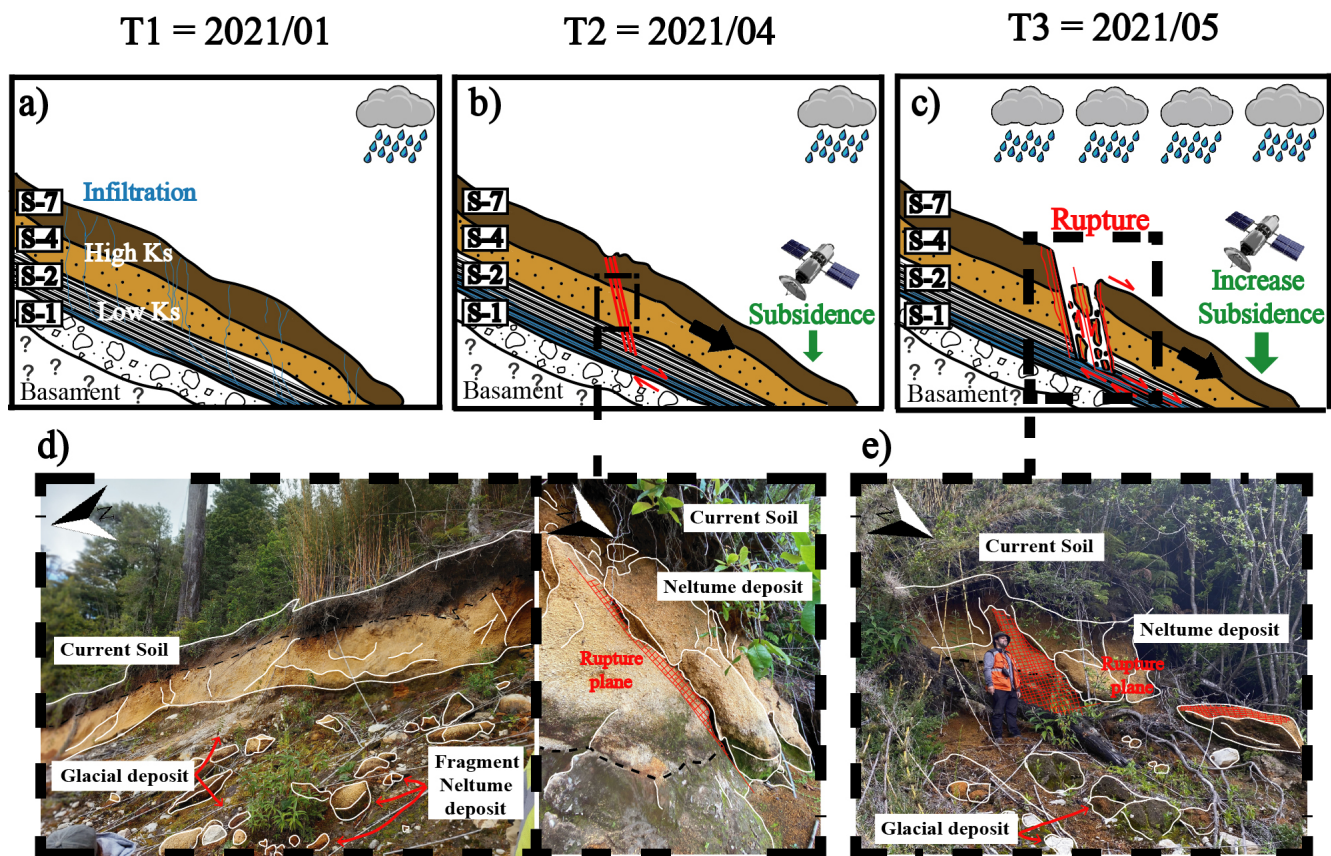


Figure 10. Conceptual model of soil deformation and following failure under cryospheric constraint. (a) First phase with low precipitation. (b) Start of the extensional failure and small-rate deformation measured by satellite. (c) Failure and initiation of the landslide and following debris flow. (d) Scarp in the crown with extensional signatures (white lines). (e) First plane of the current rupture plane that could generate new debris mass wasting.

until reaching the underlying varved glacial sediments (S-2), which have significantly lower permeability. This layering caused a perched water table, increasing the pore pressure and reducing shear strength, ultimately contributing to slope failure. These effects were captured in our remote sensing observations, which showed expanded saturated zones and local instability near the contact between volcanic and glacial deposits.

Our results suggest strong stratigraphic controls and extreme precipitation events in the soils derived from volcanic materials overlying denser glacial layers, acting as failure planes under saturated conditions (Figs. 7; 10). Our conceptual model promotes water retention and changes in soil pore pressure, especially during extreme rainfall events such as 2021 (not observed previously). The conditioning factors are further exacerbated by mid-term climate trends, including the ongoing megadrought in the Southern Andes (Garreaud et al., 2019), which increased desiccation cracking, and weakened root cohesion. Such drought-induced degradation lowers slope resistance, making even moderate precipitation more hazardous. Therefore, our observations sug-

gest that the Ñisoleufu debris flow event, may exemplify the climate-induced changes in both hydrological extremes and landscape memory (drought legacy) act in concert to reduce slope stability. As extreme precipitation becomes more frequent under future climate scenarios, similar failures are expected to occur across a broader area than observed in past events (Fig. 2A). Our findings stress the urgent need for debris flow forecasting models to incorporate stratified soil behavior, seasonal soil moisture dynamics, and drought-related weakening – factors essential to anticipating the growing hazard posed by climate change (Iverson et al., 2010; Gariano and Guzzetti, 2016).

5.3 Regional implications and Future Scope

The Southern Volcanic Zone (37.5–41.5° S; Stern 2004) has been shaped by significant volcanic Holocene eruptions (Fontaine et al., 2021; Moreno-Yaeger et al., 2024; Singer et al., 2024), leading to the formation of soils primarily composed of lapilli and/or ashes that settled following the contours of the topography, resulting in layers with varying thicknesses (Stern, 2007). Old deposits in the zone show sim-

ilarities to the current debris flow deposits (Figs. 5B; 10a), suggesting that the event triggered in 2021 is not an isolated occurrence in the area. This evidence points to a history of recurring debris flow events in the region. This condition is dominant in all the surroundings of the Mocho-Choshuenco volcanic complex (Rawson et al., 2015; Moreno-Yaeger et al., 2024).

The Ñisoleufu debris flow exhibited a characteristic pattern of mass-wasting processes in the Southern Andes, similar to the Petrohué event (Fustos-Toribio et al., 2021) at Osorno Volcano (Fig. 1D), which can be attributed to comparable climatic and volcanic conditions. The occurrence of debris flows in the Southern Andes, particularly in the border of the maximum extension of the Patagonian ice sheet suggest that debris flows are typically related to saturated soils that can transform into more fluidic mixtures. Our observations and previous studies (Davies et al., 2020; Fustos-Toribio et al., 2021) proposes a strong correlation between debris flows and glacial moraines, particularly where the last glacial maximum shaped the relief (Fig. 1B and C). The interaction of past glacial dynamics with contemporary environmental processes related to new precipitation patterns provides a backdrop for increased debris flow activities in Southern Andes based on rainfall-induced mass wasting data from Fustos-Toribio et al. (2022). Stand out regions at the borders of these past glaciers tend to exhibit increased susceptibility to debris flow generation due to the combination of steep slopes and the prevalence of loose moraine deposits (Fig. 10), which can be mobilized during significant precipitation events (Sepúlveda et al., 2014).

Our results show that precursory signals such as small progressive deformation of the surface (Fig. 10) could suggest the indication of possible soil slides previous to initiation of the debris flow (Fig. 10). This phenomenon is influenced by fine soil interspersed with glacial deposits, superimposed on moraines and volcanic deposits, common throughout the southern Andean region (Moreno-Yaeger et al., 2024; Singer et al., 2024). A simple geomorphological generalization highlights the necessity of investigating the interaction between glacial and volcanic deposits to understand better the interplay between media with constraints on soil hydraulic conductivity. Future studies should prioritise examining these dynamics to prevent and mitigate potential risks associated with similar landslide events across the broad area of the Southern Andes.

Debris flow generation in volcanic soils and their correlation with post-glacial eruptions, assumes a critical importance in comprehending the mass wasting hazards under the current climate crisis. Holocene eruptions, known for their Plinian events such as Mocho-Choshuenco, Carran-Los Venados, Calbuco, Chaitén in the Southern Andes (Singer et al., 2024), have yielded abundant tephra and volcanic soils possessing high hydraulic conductivity. These eruptions formed volcanic deposits over moraine and varve deposits (Fig. 4). The volcanic soil acts as a high-rate infiltration layer

meanwhile, the moraine crowned by impermeable varve layers in the base of the sequence plays a reservoir on (Fig. 10). Therefore, the amalgamation of these deposits with intense precipitation events may expedite the loading of these reservoirs, heightening the probability of slope instability due to increased mechanical load and pore-stress changes (Bogaard and Greco, 2015). Early indications of this phenomenon are evident in occurrences such as Choclo 2023, and Volcán Osorno (every year), suggesting a potentially heightened recurrence in the future. To mitigate the associated risks effectively, it is imperative to enhance the zoning of areas prone to debris flows in the Southern Andes, thus minimizing the impact on population and infrastructure within these vulnerable zones.

On a regional scale, climate change is intensifying debris flow hazards (Gariano and Guzzetti, 2016). In the Southern Andes, current changes in precipitation patterns will affect the stability of volcanic and glacial deposits through alterations in water storage, as noted in this study (Fig. 8B). The region's unique stratigraphy in South America, where volcanic soils overlay glacial sediments, may become unstable during extreme rainfall events. Significant shifts in precipitation patterns, as predicted by CMIP6 models, alter the spatial distribution of precipitation and their impact on soil moisture storage, with limited accurate estimations (Salazar et al., 2023). We propose that future developments should carefully constrain areas with high susceptibility to debris flow. Therefore, improved hazard debris flow delimitation and instrumental monitoring become critical for reducing the impact of these hazards in the Southern Andes.

Our study contributes to understanding the relationship between volcanic and glacial deposits under extreme rainfall events forcing in the Southern Andes. However, further research is necessary to improve the rainfall-induced mass wasting susceptibility models due to an incomplete integration of critical soil properties. Several studies focus on rainfall thresholds as primary trigger, oversimplifying the failure mechanisms. Our study proposes that additional assessment of the hydraulic and mechanical influence of specific soil layers must be considered. Additionally, the pronounced spatial heterogeneity in soil layer composition in Southern Andes, ranging from S-1 to S-7, and variability in thickness and permeability, further complicates predictive accuracy to regional scale. Future developments must consider high-resolution subsurface mapping introducing national scale models (Dinamarca et al., 2023), allowing better mass wasting risk models overlooking zones where possible saturated soil could appear, leading to sudden failure. Moreover, surface deformation frequently observed as a slow extensional signal prior to collapse introduces a limited amount of PS. Moreover, the hydrometeorological variability indicates that better soil moisture models are necessary in the zone to improve the slope stability analysis. Together, these limitations highlight the urgent need for multidisciplinary ap-

proaches that integrate geotechnical, geomorphological, and hydrometeorological data into landslide hazard assessments.

Our study proposes considerations that must be assessed in landslide research in the Southern Andes, allowing a deep understanding of the interplay between geomorphological, geotechnics, hydrometeorological and remote sensing analysis, allowing a better landslide risk assessment and mitigation efforts in the region. We propose that the Ñisoleufu event could as study case for researchers and authorities can better comprehend the specific conditions that lead to debris-flow occurrences and implement appropriate measures to minimize the impact of such events in the future. Finally, these results suggest that hazard assessment protocols should include hydrogeotechnical mapping of tephra-over-moraine systems, combined with seasonal soil moisture dynamics and weather forecasts of extreme rainfall as early indicators of instability in these settings.

6 Conclusions

We studied the conditions that evolved in the generation of debris flows in the Southern Andes, an area modulated by the glacial and volcanic processes. The mass wasting could be influenced by complex interactions among geomorphological, geotechnical, and hydrometeorological factors (Fig. 10). The geological environment of the Southern Andes, characterized by a mix of volcanic and glacial deposits, showcases unique soil properties affecting overall slope stability. The mechanisms leading to mass wasting, particularly the Ñisoleufu event, underscore the critical roles of soil saturation and effective stress reduction in triggering slope failures (Fig. 10). The analysis of geomorphological factors revealed that slopes greater than 30° significantly contribute to debris flow triggers, supporting the emphasis of rainfall's role in mass wasting (Fig. 5). The orientation of these slopes, particularly aspects with more rainfall exposure, promotes precipitation accumulation from extreme weather patterns. Our findings corroborate the influence of gradual accumulation of subsurface water, aided by low hydraulic conductivity from underlying soil layers (Fig. 7), can create critical saturation levels that reduce shear strength and lead to flow initiation. These processes, not considered in detail must be integrated in future assessment in detail into the future.

We conclude that recurrence of mass wasting is influenced by past volcanic eruptions and post-glacial conditions. A comprehensive understanding of the interplay between geological and hydrometeorological conditions is crucial for forecasting debris flow risks in the Southern Andes, particularly considering climate change, which may exacerbate extreme weather events. We highlight that while frictional soils can provide stability under dry conditions, they become increasingly vulnerable to failure under saturated conditions as was evidenced in the Ñisoleufu event. The data indicating surface deformation prior to debris flow events

(Fig. 9), demonstrating that precursory signals that can be leveraged for early warning systems. The velocity of surface movements preceding the Ñisoleufu event are correlated with increased soil moisture levels, emphasizing the utility of integrating remote sensing technologies to monitor these changes as proxy. Our findings could be extended to regional scale as a conceptual model of the landslides and debris flows in the Southern Andes, suggesting areas prone to such occurrences and should be monitored closely to develop effective mitigation strategies. Finally, our results demonstrate the value of integrating geomorphological, hydrometeorological, and hydrogeotechnical data to support debris-flow hazard assessments. In particular, the combination of tephra layers overlying low-permeability glacial deposits, together with rapid water infiltration on steep slopes during extreme rainfall events, defines a critical configuration that enhances susceptibility to failure. This integrated framework provides a robust basis for identifying high-risk areas and strengthening early warning strategies in the Southern Andes and comparable volcanic-glacial settings worldwide.

Code availability. All the codes used in this manuscript are reproducible from the main text. We can deliver the main script under any request.

Data availability. The datasets used in this study are available in the paper. The ALOS-PALSAR DEM is publicly accessible at <https://search.asf.alaska.edu/#/?dataset=ALOS> (last access: 30 September 2024). Additional information about the information or datasets can be obtained from Ivo Fustos-Toribio (ivo.fustos@ufrontera.cl).

Author contributions. IF, DB, AB, GF and AG contributed to the conceptualisation and methodology of the research and performed the formal analysis, visualisation and validation. IF and DB were involved in the funding and supervision of the paper. IF and AB contributed with the supervision, review and editing of the paper. SS and JLP contributed to the discussion of the scientific results. All the authors provided input in terms of methodology and the review and editing of the paper.

Competing interests. The contact author has declared that none of the authors has any competing interests.

Disclaimer. Publisher's note: Copernicus Publications remains neutral with regard to jurisdictional claims made in the text, published maps, institutional affiliations, or any other geographical representation in this paper. While Copernicus Publications makes every effort to include appropriate place names, the final responsibility lies with the authors. Views expressed in the text are those of the authors and do not necessarily reflect the views of the publisher.

Special issue statement. This article is part of the special issue “The influence of landslide inventory quality on susceptibility and hazard map reliability”. It is a result the EGU General Assembly 2024, session NH3.10 “Exploring the Interplay: Quality of Landslide Inventories and reliability of Susceptibility and Hazard mapping”, Vienna, Austria, 19 April 2024.

Acknowledgements. The authors gratefully acknowledge the financial support of the “Agencia Nacional de Investigación y Desarrollo (ANID)” of the Chilean Government, “Fondecyt Regular”, “Fondecyt post-doctoral” and CIVUR-39° “Centro Interactivo Vulcanológico de La Araucanía” Project UFRO2193 of the Desarrollo de Actividades de Interés Nacional (ADAIN), Ministry of Education, Chilean Government. We appreciate the support of Mauricio Hermosilla for their support in geotechnical analysis.

Financial support. This work has been supported by the “Agencia Nacional de Investigación y Desarrollo (ANID)” of the Chilean Government; “Fondecyt Regular” (grant 1230792); “FONDEF ID23i10118”; “Fondecyt post-doctoral” (grant 3200387) and CIVUR-39° “Centro Interactivo Vulcanológico de La Araucanía” Project UFRO2193 of the Desarrollo de Actividades de Interés Nacional (ADAIN), Ministry of Education, Chilean Government.

Review statement. This paper was edited by Lorenzo Nava and reviewed by two anonymous referees.

References

- Bekaert, D. P. S., Walters, R. J., Wright, T. J., Hooper, A. J., and Parker, D. J.: Statistical comparison of InSAR tropospheric correction techniques, *Remote Sens. Environ.*, 170, 40–47, <https://doi.org/10.1016/j.rse.2015.08.035>, 2015.
- Bogaard, T. A. and Greco, R.: Landslide hydrology: from hydrology to pore pressure, *WIREs Water*, 3, 439–459, <https://doi.org/10.1002/wat.2.1126>, 2015.
- Bordoni, M., Vivaldi, V., Ciabatta, L., Brocca, L., and Meisina, C.: Temporal prediction of shallow landslides exploiting soil saturation degree derived by ERA5-Land products, *B. Eng. Geol. Environ.*, 82, <https://doi.org/10.1007/s10064-023-03304-2>, 2023.
- Bovis, M. J. and Jakob, M.: The role of debris supply conditions in predicting debris flow activity, *Earth Surf. Proc. Land.*, 24, 1039–1054, [https://doi.org/10.1002/\(SICI\)1096-9837\(199910\)24:11<1039::AID-ESP29>3.0.CO;2-U](https://doi.org/10.1002/(SICI)1096-9837(199910)24:11<1039::AID-ESP29>3.0.CO;2-U), 1999.
- Bucher, J., del Papa, C., Hernando, I. R., and Almada, G.: Upper-flow-regime deposits related to glacio-volcanic interactions in Patagonia: Insights from the Pleistocene record in Southern Andes, *Sedimentology*, 71, 2314–2334, <https://doi.org/10.1111/sed.13216>, 2024.
- Carrasco, F. and Ramírez, P.: Caracterización de remociones en masa del 31 de mayo de 2021, en la ribera sur del Lago Calafquén, sobre la Ruta CH-201, Comuna de Panguipulli, Región de Los Ríos, Informe inédito, INF-LOS RÍOS-09.2021, Subdirección Nacional De Geología, Sernageomin, Stgo, Chile, 23 pp., 2021.
- Chang, J.-M., Chen, H., Jou, B. J.-D., Tsou, N.-C., and Lin, G.-W.: Characteristics of rainfall intensity, duration, and kinetic energy for landslide triggering in Taiwan, *Engineering Geology*, 231, 81–87, <https://doi.org/10.1016/j.enggeo.2017.10.006>, 2017.
- Chang, J.-M., Yang, C.-M., Chao, W.-A., Ku, C.-S., Huang, M.-W., Hsieh, T.-C., and Hung, C.-Y.: Unraveling landslide failure mechanisms with seismic signal analysis for enhanced pre-survey understanding, *Nat. Hazards Earth Syst. Sci.*, 25, 451–466, <https://doi.org/10.5194/nhess-25-451-2025>, 2025.
- Chen, Y., Lin, H., Cao, R., and Zhang, C.: Slope Stability Analysis Considering Different Contributions of Shear Strength Parameters, *Int. J. Geomech.*, 21, [https://doi.org/10.1061/\(asce\)gm.1943-5622.0001937](https://doi.org/10.1061/(asce)gm.1943-5622.0001937), 2021.
- Chen, Y.-W., Shyu, J. B. H., and Chang, C.-P.: Neotectonic characteristics along the eastern flank of the Central Range in the active Taiwan orogen inferred from fluvial channel morphology, *Tectonics*, 34, 2249–2270, <https://doi.org/10.1002/2014tc003795>, 2015.
- Cheung, D. J. and Giardino, J. R.: Debris flow occurrence under changing climate and wildfire regimes: A southern California perspective, *Geomorphology*, 422, 108538, <https://doi.org/10.1016/j.geomorph.2022.108538>, 2023.
- Cui, P., Zhu, Y., Han, Y., Chen, X., and Zhuang, J.: The 12 May Wenchuan earthquake-induced landslide lakes: distribution and preliminary risk evaluation, *Landslides*, 6, 209–223, <https://doi.org/10.1007/s10346-009-0160-9>, 2009.
- Dahal, R. K. and Hasegawa, S.: Representative rainfall thresholds for landslides in the Nepal Himalaya, *Geomorphology*, 100, 429–443, <https://doi.org/10.1016/j.geomorph.2008.01.014>, 2008.
- Dahal, R. K., Hasegawa, S., Yamanaka, M., and Bhandary, N. P.: Rainfall-induced landslides in the residual soil of andesitic terrain, western Japan, *Journal of Nepal Geological Society*, 42, 137–152, <https://doi.org/10.3126/jngs.v42i0.31461>, 2011.
- Dane, J. H. and Clarke Topp, G. (Eds.): *Methods of Soil Analysis*, SSSA Book Series, <https://doi.org/10.2136/sssabookser5.4>, 2002.
- Davies, B. J., Darvill, C. M., Lovell, H., Bendle, J. M., Dowdeswell, J. A., Fabel, D., García, J.-L., Geiger, A., Glasser, N. F., Gheorghiu, D. M., Harrison, S., Hein, A. S., Kaplan, M. R., Martin, J. R. V., Mendelova, M., Palmer, A., Peltó, M., Rodés, Á., Sagredo, E. A., Smedley, R. K., Smellie, J. L., and Thorndy-craft, V. R.: The evolution of the Patagonian Ice Sheet from 35 ka to the present day (PATICE), *Earth-Sci. Rev.*, 204, 103152, <https://doi.org/10.1016/j.earscirev.2020.103152>, 2020.
- Deng, Y., Cai, C., Xia, D., Ding, S., Chen, J., and Wang, T.: Soil Atterberg limits of different weathering profiles of the collapsing gullies in the hilly granitic region of southern China, *Solid Earth*, 8, 499–513, <https://doi.org/10.5194/se-8-499-2017>, 2017.
- De Pue, J., Rezaei, M., Van Meirvenne, M., and Cornelis, W. M.: The relevance of measuring saturated hydraulic conductivity: Sensitivity analysis and functional evaluation, *J. Hydrol.*, 576, 628–638, <https://doi.org/10.1016/j.jhydrol.2019.06.079>, 2019.
- Dey, N. and Sengupta, A.: Effect of rainfall on the triggering of the devastating slope failure at Malin, India, *Nat. Hazards*, 94, 1391–1413, <https://doi.org/10.1007/s11069-018-3483-9>, 2018.
- Dinamarca, D. I., Galleguillos, M., Seguel, O., and Faúndez Urbina, C.: CLSoilMaps: A national soil gridded database of physical and hydraulic soil properties for Chile, *Sci. Data*, 10, <https://doi.org/10.1038/s41597-023-02536-x>, 2023.

- Ferretti, A., Prati, C., and Rocca, F.: Permanent scatterers in SAR interferometry, *IEEE T. Geosci. Remote*, 39, 8–20, <https://doi.org/10.1109/36.898661>, 2001.
- Fiantis, D., Ginting, F., Gusnidar, Nelson, M., and Minasny, B.: Volcanic Ash, Insecurity for the People but Securing Fertile Soil for the Future, *Sustainability*, 11, 3072, <https://doi.org/10.3390/su11113072>, 2019.
- Fontaine, C. M., Siani, G., Delpéch, G., Michel, E., Villarosa, G., Manssouri, F., and Nouet, J.: Post-glacial tephrochronology record off the Chilean continental margin ($\sim 41^\circ\text{S}$), *Quaternary Sci. Rev.*, 261, 106928, <https://doi.org/10.1016/j.quascirev.2021.106928>, 2021.
- Foumelis, M., Delgado Blasco, J. M., Desnos, Y.-L., Engdahl, M., Fernandez, D., Veci, L., Lu, J., and Wong, C.: Esa Snap - Stamps Integrated Processing for Sentinel-1 Persistent Scatterer Interferometry, *IGARSS 2018 - 2018 IEEE International Geoscience and Remote Sensing Symposium*, <https://doi.org/10.1109/igarss.2018.8519545>, 2018.
- Funk, C., Peterson, P., Landsfeld, M., Pedreros, D., Verdin, J., Shukla, S., Husak, G., Rowland, J., Harrison, L., Hoell, A., and Michaelsen, J.: The climate hazards infrared precipitation with stations – a new environmental record for monitoring extremes, *Sci Data*, 2, <https://doi.org/10.1038/sdata.2015.66>, 2015.
- Fustos, I., Remy, D., Abarca-Del-Rio, R., and Muñoz, A.: Slow movements observed within situ and remote-sensing techniques in the central zone of Chile, *Int. J. Remote Sens.*, 38, 7514–7530, <https://doi.org/10.1080/01431161.2017.1317944>, 2017.
- Fustos, I., Abarca-del-Rio, R., Moreno-Yaeger, P., and Somos-Valenzuela, M.: Rainfall-Induced Landslides forecast using local precipitation and global climate indexes, *Nat. Hazards*, 102, 115–131, <https://doi.org/10.1007/s11069-020-03913-0>, 2020a.
- Fustos, I., Abarca-del-Río, R., Mardones, M., González, L., and Araya, L. R.: Rainfall-induced landslide identification using numerical modelling: A southern Chile case, *J. S. Am. Earth Sci.*, 101, 102587, <https://doi.org/10.1016/j.jsames.2020.102587>, 2020b.
- Fustos-Toribio, I. J., Morales-Vargas, B., Somos-Valenzuela, M., Moreno-Yaeger, P., Muñoz-Ramirez, R., Rodriguez Araneda, I., and Chen, N.: Debris flow event on Osorno volcano, Chile, during summer 2017: new interpretations for chain processes in the southern Andes, *Nat. Hazards Earth Syst. Sci.*, 21, 3015–3029, <https://doi.org/10.5194/nhess-21-3015-2021>, 2021.
- Fustos-Toribio, I., Manque-Roa, N., Vásquez Antipán, D., Hermosilla Sotomayor, M., and Letelier Gonzalez, V.: Rainfall-induced landslide early warning system based on corrected mesoscale numerical models: an application for the southern Andes, *Nat. Hazards Earth Syst. Sci.*, 22, 2169–2183, <https://doi.org/10.5194/nhess-22-2169-2022>, 2022.
- Galetto, F., Pritchard, M. E., Hornby, A. J., Gazel, E., and Mahowald, N. M.: Spatial and Temporal Quantification of Subaerial Volcanism From 1980 to 2019: Solid Products, Masses, and Average Eruptive Rates, *Rev. Geophys.*, 61, <https://doi.org/10.1029/2022rg000783>, 2023.
- Gariano, S. L. and Guzzetti, F.: Landslides in a changing climate, *Earth-Sci. Rev.*, 162, 227–252, <https://doi.org/10.1016/j.earscirev.2016.08.011>, 2016.
- Garreaud, R. D., Boisier, J. P., Rondanelli, R., Montecinos, A., Sepúlveda, H. H., and Veloso-Aguila, D.: The Central Chile Mega Drought (2010–2018): A climate dynamics perspective, *Int. J. Climatol.*, 40, 421–439, <https://doi.org/10.1002/joc.6219>, 2019.
- Gregoretti, C.: The initiation of debris flow at high slopes: experimental results, *J. Hydraul. Res.*, 38, 83–88, <https://doi.org/10.1080/00221680009498343>, 2000.
- Hooper, A.: A multi-temporal InSAR method incorporating both persistent scatterer and small baseline approaches, *Geophys. Res. Lett.*, 35, <https://doi.org/10.1029/2008gl034654>, 2008.
- Hooper, A., Segall, P., and Zebker, H.: Persistent scatterer interferometric synthetic aperture radar for crustal deformation analysis, with application to Volcán Alcedo, Galápagos, *J. Geophys. Res.*, 112, <https://doi.org/10.1029/2006jb004763>, 2007.
- Hooper, A., Bekaert, D., Spaans, K., and Arkan, M.: Recent advances in SAR interferometry time series analysis for measuring crustal deformation, *Tectonophysics*, 514–517, 1–13, <https://doi.org/10.1016/j.tecto.2011.10.013>, 2012.
- Höser, T.: Analysing the capabilities and limitations of InSAR using Sentinel-1 data for landslide detection and monitoring, PhD diss., University of Bonn, 2018.
- Huang, A.-B., Lee, J.-T., Ho, Y.-T., Chiu, Y.-F., and Cheng, S.-Y.: Stability monitoring of rainfall-induced deep landslides through pore pressure profile measurements, *Soils and Foundations*, 52, 737–747, <https://doi.org/10.1016/j.sandf.2012.07.013>, 2012.
- Hungr, O., Leroueil, S., and Picarelli, L.: The Varnes classification of landslide types, an update, *Landslides*, 11, 167–194, <https://doi.org/10.1007/s10346-013-0436-y>, 2014.
- Iverson, R., Logan, M., LaHusen, R., and Berti, M.: The perfect debris flow? Aggregated results from 28 large-scale experiments, *J. Geophys. Res.-Atmos.*, 115, F03005, <https://doi.org/10.1029/2009jf001514>, 2010.
- Jakob, M. und Lambert, S.: Climate change effects on landslides along the southwest coast of British Columbia, *Geomorphology*, 107, 275–284, <https://doi.org/10.1016/j.geomorph.2008.12.009>, 2009.
- Kameda, J., Kamiya, H., Masumoto, H., Morisaki, T., Hiratsuka, T., and Inaoi, C.: Fluidized landslides triggered by the liquefaction of subsurface volcanic deposits during the 2018 Ibuli–Tobu earthquake, Hokkaido, *Sci. Rep.*, 9, <https://doi.org/10.1038/s41598-019-48820-y>, 2019.
- Kang, D., Nam, D., Lee, S., Yang, W., You, K., and Kim, B.: Comparison of impact forces generated by debris flows using numerical analysis models, *WIT Trans. Ecol. Env.*, 220, 195–203, <https://doi.org/10.2495/wrm170191>, 2017.
- Kinde, M., Getahun, E., and Jothamani, M.: Geotechnical and slope stability analysis in the landslide-prone area: A case study in Sawla – Laska road sector, Southern Ethiopia, *Scientific African*, 23, e02071, <https://doi.org/10.1016/j.sciaf.2024.e02071>, 2024.
- Korup, O., Seidemann, J., and Mohr, C. H.: Increased landslide activity on forested hillslopes following two recent volcanic eruptions in Chile, *Nat. Geosci.*, 12, 284–289, <https://doi.org/10.1038/s41561-019-0315-9>, 2019.
- Kuriakose, S. L., van Beek, L. P. H., and van Westen, C. J.: Parameterizing a physically based shallow landslide model in a data poor region, *Earth Surf. Proc. Land.*, 34, 867–881, <https://doi.org/10.1002/esp.1794>, 2009.
- Lee, C.-T.: Landslide trends under extreme climate events, *Terr. Atmos. Ocean. Sci.*, 28, 33–42, [https://doi.org/10.3319/tao.2016.05.28.01\(cca\)](https://doi.org/10.3319/tao.2016.05.28.01(cca)), 2017.

- Malet, J.-P., Laigle, D., Remaître, A., and Maquaire, O.: Triggering conditions and mobility of debris flows associated to complex earthflows, *Geomorphology*, 66, 215–235, <https://doi.org/10.1016/j.geomorph.2004.09.014>, 2005.
- Maragaño-Carmona, G., Fustos Toribio, I. J., Descote, P.-Y., Robledo, L. F., Villalobos, D., and Gatica, G.: Rainfall-Induced Landslide Assessment under Different Precipitation Thresholds Using Remote Sensing Data: A Central Andes Case, *Water*, 15, 2514, <https://doi.org/10.3390/w15142514>, 2023.
- Moreno-Yaeger, P., Singer, B. S., Edwards, B. R., Jicha, B. R., Nachlas, W. O., Kurz, M. D., E. Breunig, R., Fustos-Toribio, I., Antipán, D. V., and Piergrossi, E.: Pleistocene to recent evolution of Mocho-Choshuenco volcano during growth and retreat of the Patagonian Ice Sheet, *Geological Society of America Bulletin*, 136, 5262–5282, <https://doi.org/10.1130/b37514.1>, 2024.
- Muñoz-Sabater, J., Dutra, E., Agustí-Panareda, A., Albergel, C., Arduini, G., Balsamo, G., Boussetta, S., Choulga, M., Harri-gan, S., Hersbach, H., Martens, B., Miralles, D. G., Piles, M., Rodríguez-Fernández, N. J., Zsoter, E., Buontempo, C., and Thépaut, J.-N.: ERA5-Land: a state-of-the-art global reanalysis dataset for land applications, *Earth Syst. Sci. Data*, 13, 4349–4383, <https://doi.org/10.5194/essd-13-4349-2021>, 2021.
- Muratli, J. M., Chase, Z., McManus, J., and Mix, A.: Ice-sheet control of continental erosion in central and southern Chile (36°–41°S) over the last 30,000 years, *Quaternary Sci. Rev.*, 29, 3230–3239, <https://doi.org/10.1016/j.quascirev.2010.06.037>, 2010.
- Ochoa-Cornejo, F., Palma, S., Sepúlveda, S. A., Lara, M., Burgos, K., and Duhart, P.: Rock slides in paraglacial environments in South America: three-dimensional modeling of glacier retreat and landslide inducing the 2017 Santa Lucía disaster in the Chilean Patagonia, *Landslides*, 22, 1003–1025, <https://doi.org/10.1007/s10346-024-02419-1>, 2024.
- Ontiveros-Ortega, A., Plaza, I., Calero, J., Moleon, J. A., and Ibáñez, J. M.: High variability of interaction energy between volcanic particles: implications for deposit stability, *Nat Hazards*, 117, 3103–3122, <https://doi.org/10.1007/s11069-023-05979-y>, 2023.
- Palazzolo, N., Peres, D. J., Creaco, E., and Cancelliere, A.: Using principal component analysis to incorporate multi-layer soil moisture information in hydrometeorological thresholds for landslide prediction: an investigation based on ERA5-Land reanalysis data, *Nat. Hazards Earth Syst. Sci.*, 23, 279–291, <https://doi.org/10.5194/nhess-23-279-2023>, 2023.
- Pavlova, I., Jomelli, V., Brunstein, D., Grancher, D., Martin, E., and Déqué, M.: Debris flow activity related to recent climate conditions in the French Alps: A regional investigation, *Geomorphology*, 219, 248–259, <https://doi.org/10.1016/j.geomorph.2014.04.025>, 2014.
- Porchet, M. and Laferrere, H.: Détermination des caractéristiques hydrodynamiques des sols en place. Mémoire et notes techniques, *Ann. Du Ministère de l'Agriculture, Tech. Rep.* 2 (64), 1935.
- Rawson, H., Naranjo, J. A., Smith, V. C., Fontijn, K., Pyle, D. M., Mather, T. A., and Moreno, H.: The frequency and magnitude of post-glacial explosive eruptions at Volcán Mocho-Choshuenco, southern Chile, *J. Volcanol. Geoth. Res.*, 299, 103–129, <https://doi.org/10.1016/j.jvolgeores.2015.04.003>, 2015.
- Rodríguez, C., Perez, Y., Hugo Roa, Clayton, J., Antinao, J. L., & Duhart, P., Martin, M.: Geología del área de Panguipulli-Riñihue, Región de Los Lagos, Servicio Nacional de Geología y Minería, Mapas Geológicos No: 10, 1999.
- Salazar, Á., Thatcher, M., Goubanova, K., Bernal, P., Gutiérrez, J., and Squeo, F.: CMIP6 precipitation and temperature projections for Chile, *Clim. Dynam.*, 62, 2475–2498, <https://doi.org/10.1007/s00382-023-07034-9>, 2023.
- Sanhueza, C., Palma, J., Valenzuela, P., Araneda, O., and Calderón, K.: Evaluación del comportamiento geotécnico de suelos volcánicos chilenos para su uso como material de filtro en la depuración de aguas residuales domésticas, *Revista de la Construcción*, 10, 66–81, <https://doi.org/10.4067/s0718-915x2011000200007>, 2011.
- Savi, S., Schildgen, T. F., Tofelde, S., Wittmann, H., Scherler, D., Mey, J., Alonso, R. N., and Strecker, M. R.: Climatic controls on debris-flow activity and sediment aggradation: The Del Medio fan, NW Argentina, *J. Geophys. Res.-Earth*, 121, 2424–2445, <https://doi.org/10.1002/2016jf003912>, 2016.
- Schmidt, K. M., Roering, J. J., Stock, J. D., Dietrich, W. E., Montgomery, D. R., and Schaub, T.: The variability of root cohesion as an influence on shallow landslide susceptibility in the Oregon Coast Range, *Can. Geotech. J.*, 38, 995–1024, <https://doi.org/10.1139/t01-031>, 2001.
- Sepúlveda, S. A.: Large volume landslides in the central andes of Chile and Argentina (32°–34°S) and related hazards, *Italian Journal of Engineering Geology and Environment*, 287–294, <https://doi.org/10.4408/IJEGE.2013-06.B-26>, 2013.
- Sepúlveda, S. A. and Padilla, C.: Rain-induced debris and mudflow triggering factors assessment in the Santiago cordilleran foothills, Central Chile, *Nat. Hazards*, 47, 201–215, <https://doi.org/10.1007/s11069-007-9210-6>, 2008.
- Sepúlveda, S. A. and Petley, D. N.: Regional trends and controlling factors of fatal landslides in Latin America and the Caribbean, *Nat. Hazards Earth Syst. Sci.*, 15, 1821–1833, <https://doi.org/10.5194/nhess-15-1821-2015>, 2015.
- Sepúlveda, S. A., Moreiras, S. M., Lara, M., and Alfaro, A.: Debris flows in the Andean ranges of central Chile and Argentina triggered by 2013 summer storms: characteristics and consequences, *Landslides*, 12, 115–133, <https://doi.org/10.1007/s10346-014-0539-0>, 2014.
- Singer, B. S., Moreno-Yaeger, P., Townsend, M., Huber, C., Cuzzone, J., Edwards, B. R., Romero, M., Orellana-Salazar, Y., Marcott, S. A., Breunig, R. E., Ferrier, K. L., Scholz, K., Coonin, A. N., Alloway, B. V., Tremblay, M. M., Stevens, S., Fustos-Toribio, I., Moreno, P. I., Vera, F., and Amigo, Á.: New perspectives on ice forcing in continental arc magma plumbing systems, *J. Volcanol. Geoth. Res.*, 455, 108187, <https://doi.org/10.1016/j.jvolgeores.2024.108187>, 2024.
- Singh, K. and Kumar, V.: Rainfall Thresholds Triggering Landslides: A Review, *Lecture Notes in Civil Engineering*, 455–464, https://doi.org/10.1007/978-3-030-51354-2_42, 2020.
- Somos-Valenzuela, M. A., Oyarzún-Ulloa, J. E., Fustos-Toribio, I. J., Garrido-Urzu, N., and Chen, N.: The mudflow disaster at Villa Santa Lucía in Chilean Patagonia: understandings and insights derived from numerical simulation and postevent field surveys, *Nat. Hazards Earth Syst. Sci.*, 20, 2319–2333, <https://doi.org/10.5194/nhess-20-2319-2020>, 2020.
- Stern, C. R.: Active Andean volcanism: its geologic and tectonic setting, *Rev. Geol. Chile*, 31, <https://doi.org/10.4067/s0716-02082004000200001>, 2004.

- Stern, C. R.: Holocene tephrochronology record of large explosive eruptions in the southernmost Patagonian Andes, *B. Volcanol.*, 70, 435–454, <https://doi.org/10.1007/s00445-007-0148-z>, 2007.
- Stoffel, M., Mendlik, T., Schneuwly-Bollschweiler, M., and Go-biet, A.: Possible impacts of climate change on debris-flow activity in the Swiss Alps, *Climatic Change*, 122, 141–155, <https://doi.org/10.1007/s10584-013-0993-z>, 2013.
- Talebi, A., Uijlenhoet, R., and Troch, P. A.: Soil moisture storage and hillslope stability, *Nat. Hazards Earth Syst. Sci.*, 7, 523–534, <https://doi.org/10.5194/nhess-7-523-2007>, 2007.
- Thompson, P. I. J., Dugmore, A. J., Newton, A. J., Cutler, N. A., and Streeter, R. T.: The influence of burial rate on variability in tephra thickness and grain size distribution in Iceland, *CATENA*, 225, 107025, <https://doi.org/10.1016/j.catena.2023.107025>, 2023.
- Valenzuela, R. A. and Garreaud, R. D.: Extreme Daily Rainfall in Central-Southern Chile and Its Relationship with Low-Level Horizontal Water Vapor Fluxes, *J. Hydrometeorol.*, 20, 1829–1850, <https://doi.org/10.1175/jhm-d-19-0036.1>, 2019.
- Vásquez-Antipán, D., Fustos-Toribio, I., Riffo-López, J., Cortez-Díaz, A., Bravo, Á., and Moreno-Yaeger, P.: Landslide processes related to recurrent explosive eruptions in the Southern Andes of Chile (39° S), *J. S. Am. Earth Sci.*, 157, 105469, <https://doi.org/10.1016/j.jsames.2025.105469>, 2025.
- Vega, J. A. and Hidalgo, C. A.: Quantitative risk assessment of landslides triggered by earthquakes and rainfall based on direct costs of urban buildings, *Geomorphology*, 273, 217–235, <https://doi.org/10.1016/j.geomorph.2016.07.032>, 2016.
- Walding, N., Williams, R., Rowley, P., and Dowey, N.: Cohesional behaviours in pyroclastic material and the implications for deposit architecture, *B. Volcanol.*, 85, <https://doi.org/10.1007/s00445-023-01682-9>, 2023.
- Wang, H., Cui, P., Li, Y., Tang, J., Wei, R., Yang, A., Zhou, L., Bazai, N. A., and Zhang, G.: Rock and ice avalanche-generated catastrophic debris flow at Chamoli, 7 February 2021: New insights from the geomorphic perspective, *Geomorphology*, 452, 109110, <https://doi.org/10.1016/j.geomorph.2024.109110>, 2024.
- Wang, J. and Yu, Y.: Debris Flow Hazard Zoning Based on Numerical Simulation in the Wenchuan Earthquake Meizoseismal Areas, *Proceedings of the 5th International Conference on Civil Engineering and Transportation 2015*, <https://doi.org/10.2991/iccet-15.2015.81>, 2015.
- Xie, M., Zhao, W., Ju, N., He, C., Huang, H., and Cui, Q.: Landslide evolution assessment based on InSAR and real-time monitoring of a large, reactivated landslide, Wenchuan, China, *Eng. Geol.*, 277, 105781, <https://doi.org/10.1016/j.enggeo.2020.105781>, 2020.
- Yi, Z., Xingmin, M., Allesandro, N., Tom, D., Guan, C., Colm, J., Yuanxi, L., and Xiaojun, S.: Characterization of pre-failure deformation and evolution of a large earthflow using InSAR monitoring and optical image interpretation, *Landslides*, 19, 35–50, <https://doi.org/10.1007/s10346-021-01744-z>, 2021.
- Yu, C., Li, Z., Penna, N. T., and Crippa, P.: Generic Atmospheric Correction Model for Interferometric Synthetic Aperture Radar Observations, *J. Geophys. Res.-Sol. Ea.*, 123, 9202–9222, <https://doi.org/10.1029/2017jb015305>, 2018.